https://doi.org/10.5194/egusphere-2026-1613
Preprint. Discussion started: 8 April 2026

Assessment of aerosol iron (Fe) solubility using global dataset, Part I: Mechanisms underlying the inverse relationship between Fe solubility and Fe concentration

Kohei Sakata[1], Minako Kurisu[2], Yoshio Takahashi[3]

[1]Materials Science and Engineering, Graduate School of Engineering, Tokyo Denki University, 5 Senjyu-Asahi-Cho, Adachi-ku, Tokyo 120-8551, Japan.

[2]Atmosphere and Ocean Research Institute, The University of Tokyo, 5-1-5, Kashiwanoha, Kashiwa, Chiba 277-8564, Japan.

[3]Graduate School of Science, The University of Tokyo, 7-3-1, Hongo Bunkyo-ku, Tokyo 113-0033, Japan.

Corresponding author: Kohei Sakata (kohei.sakata.33@mail.dendai.ac.jp)

ORCID: 0000-0002-0103-9631

https://doi.org/10.5194/egusphere-2026-1613
Preprint. Discussion started: 8 April 2026

Abstract.

Atmospheric deposition of aerosol iron (Fe) can stimulate marine primary productivity by supplying dissolved Fe (d-Fe) to the surface ocean, thereby potentially influencing the global climate. Aerosol Fe solubility (Fe_{sol}%) is closely linked to its bioavailability, and previous studies have shown that Fe_{sol}% generally increases as aerosol Fe concentration decreases. However, the mechanism underlying this widely observed inverse relationship remains unresolved. In this study, aerosol observations from East Asia, the North and South Pacific, and the Atlantic were compiled, and the ratios of total Fe to total Al (T-Fe/T-Al) and dissolved Fe to dissolved Al ([d-Fe]/[d-Al]) were used to estimate the contributions of mineral-derived and anthropogenic Fe to aerosol d-Fe, as well as the Fe_{sol}% of each source fraction. Aerosol d-Fe was found to be derived predominantly from mineral dust in many oceanic regions. In addition, both mineral-derived Fe and anthropogenic Fe showed inverse relationships between concentration and solubility. If the inverse relationship between Fe concentration and Fe_{sol}% were controlled mainly by simple two-component mixing between low-solubility mineral particles and highly soluble anthropogenic Fe, the Fe_{sol}% of each source fraction would not be expected to vary systematically with concentration. Instead, the results suggest that atmospheric chemical processing, together with depositional removal during transport, progressively increases the solubility of Fe remaining in aerosol particles. The ability to estimate the sources and dissolution processes of aerosol Fe from such fundamental concentration data may help improve the parameterization of aerosol Fe dissolution in global climate models.

https://doi.org/10.5194/egusphere-2026-1613
Preprint. Discussion started: 8 April 2026

1 Introduction

Aerosol particles play a central role in the biogeochemical cycling of the Earth's surface environment. One key process is the fertilization of the oceans by aerosol-derived iron (Fe) (Jickells et al., 2005; Mahowald et al., 2009; Kanakidou et al., 2018). In high-nutrient, low-chlorophyll (HNLC) regions, primary production is limited by the scarcity of dissolved iron (d-Fe) in surface waters (Martin and Fitzwater, 1988; Martin, 1990; Martin et al., 1994; Boyd et al., 2007). The addition of d-Fe to these regions stimulates the biological pump, thereby influencing the cycling of carbon, nitrogen, sulfur, and Fe (Charlson et al., 1987; Krishnamurthy et al., 2009; Jin et al., 2008). Aerosols are recognized as a major source of d-Fe to the surface ocean, and numerous studies have examined this contribution (Baker et al., 2006a, 2006b, 2013, 2020; Buck et al., 2006, 2010a, 2010b, 2013; Chance et al., 2015; Shelley et al., 2018; Marsay et al., 2022; Sakata et al., 2022; Kurisu et al., 2021, 2024). These studies indicate that the fractional Fe solubility (Fe_{sol}%) in aerosols is primarily governed by (i) differences in Fe_{sol}% among emission sources (e.g., mineral dust, volcanic ash, anthropogenic aerosols) and their relative abundances, and (ii) chemical alterations, including proton-promoted, ligand-promoted, and photoreductive Fe dissolutions. However, the relative importance of these factors of Fe_{sol}% remains poorly constrained (Mahowald et al., 2009, 2018; Olgun et al., 2011; Sholkovitz et al., 2012; Ito et al., 2019; Baker et al., 2021).

Limited knowledge of the seasonal variability of Fe_{sol}% further contributes to this uncertainty. The supply of aerosol Fe from East Asia to the North Pacific is modulated by seasonal variations in both natural and anthropogenic sources. Mineral dust loading typically peaks in spring (Uematsu et al., 1983; Zhu et al., 2020; Kawai et al., 2021), whereas concentrations of several anthropogenic pollutants increase in winter due to higher residential fuel combustion (Ma et al., 2017; Zhang et al., 2018; Kurokawa and Ohara, 2020). Previous work suggests that anthropogenic Fe (anthro-Fe) generally exhibits higher Fe_{sol}% than mineral dust, implying that seasonal changes in their relative contributions influence Fe_{sol}% overall. Aerosol pH, which controls Fe dissolution rates, particularly for proton-promoted processes, also varies seasonally in response to temperature and humidity changes (Guo et al., 2016; Tao and Murphy, 2019a; Song and Osada, 2020; Pye et al., 2020; Zheng et al., 2020). Consequently, Fe_{sol}% is also expected to exhibit seasonal variability. Given that most Fe in marine aerosols originates from continental regions, long-term observations in both marine and continental atmospheres are essential for identifying the controlling factors of Fe_{sol}%. However, studies covering longer than one year are scarce, even at land-based sites, and conducting such long-term observations during research cruises is particularly challenging. Moreover, only limited attempts have been made to compile existing measurement data to systematically evaluate the seasonal variability of Fe_{sol}% and the mechanisms governing it in marine aerosols.

To understand the seasonal variability of Fe_{sol}% in aerosols collected from both terrestrial and marine atmospheres, as well as to elucidate the controlling factors, it is essential to compile existing data and discuss them in detail. This study compiled a global dataset from previous observational work and associated measurements of total and dissolved Fe and Al concentrations and their solubilities. The dataset encompasses East Asia (Duvall et al., 2008; Li et al., 2015; Kurisu et al., 2019; Hsieh et al., 2023; Sakata et al., 2023, 2025; Seo and Kim, 2023), the North Pacific (Buck et al., 2006, 2013; Marsay

https://doi.org/10.5194/egusphere-2026-1613
Preprint. Discussion started: 8 April 2026

et al., 2022; Sakata et al., 2022; Kurisu et al., 2024), the South Pacific (Buck et al., 2013, 2019; Sakata et al., 2022; Perron et al., 2020a, 2021), and the Atlantic Ocean (Baker et al., 2006a, 2006b, 2013, 2020; Buck et al., 2010a, 2010b; Chance et al., 2015). We included Al data because a plot of the enrichment factor of total Fe ($EF_{T\text{-}Fe}$ = $(T\text{-}Fe/T\text{-}Al)_{aerosol}/(T\text{-}Fe/T\text{-}Al)_{crust}$) plotted against the molar ratio of d-Fe to dissolved Al ([d-Fe]/[d-Al]) is a useful tool for identifying emission sources of T-Fe and d-Fe (Sakata et al., 2023). We first calculated monthly means of T-Fe and T-Al concentrations and solubilities to characterize seasonal variabilities. We then estimated the contribution of anthropogenic-derived d-Fe to total aerosol d-Fe, and separately evaluated the Fe_{sol}% of mineral dust and anthropogenic aerosols to assess the seasonal variability of their atmospheric alteration processes. Finally, we reanalyzed the compiled data using standardized metrics, including $EF_{T\text{-}Fe}$ and [d-Fe]/[d-Al], to investigate the factors controlling Fe_{sol}%. This reanalysis aimed both to clarify spatiotemporal patterns linked to these controlling factors and to identify key gaps that should be addressed in future observational studies.

2 Methods

2.1 Data compilation of total and dissolved Fe and Al concentrations

This study primarily utilized data reported in previous observations, supplemented by our unpublished data from size-resolved aerosol samples collected in the Pacific Ocean. Detailed descriptions of the sampling and analytical procedures for these unpublished data are provided in Section S1 of the Supplementary Information. For data compilation, only samples for which concentrations of T-Fe, T-Al, d-Fe, and d-Al were concurrently available were included. In certain studies, d-Fe and d-Al concentrations were derived based on their corresponding Fe_{sol}% or Al_{sol}%. All compiled data were acquired through filter-based collection methods. Aerosol particles were sampled using cellulose, quartz fiber, or PTFE fiber filters (Buck and Pytan, 2012; Morton et al., 2013; Sakata et al., 2018). Although the choice of filter material may influence measured Fe_{sol}% and Al_{sol}%, this effect is generally limited to a few percent, which is minor relative to the observed variability. Therefore, differences in sampling substrates were not accounted for in this study. While the majority of previous studies collected total suspended particulates (TSP), size-fractionated aerosol samples were occasionally utilized. In this study, coarse and fine aerosol particles are defined as those with aerodynamic diameters greater than or less than 2.5 μm, respectively. Samples were predominantly preserved by freezing at –20°C or by storage in a desiccator at ambient temperature under dry conditions (approximately 20% relative humidity).

Given the variability in acid digestion and extraction protocols for Fe and Al across studies, specific criteria were established for data compilation. A critical consideration was whether hydrofluoric acid (HF) was incorporated in the digestion process. It is known that the incomplete digestion of Si-O bond present in aluminosilicates, due to the omission of HF, leads to an underestimation of the T-Fe and T-Al concentrations that are substituted or trapped within it. Therefore, in this study, we only compiled, and concentrations obtained from aerosol samples digested with acids that included both

https://doi.org/10.5194/egusphere-2026-1613
Preprint. Discussion started: 8 April 2026

HNO_3 and HF, following the methodology of Morton et al. (2013). These elemental concentrations were primarily determined by inductively coupled plasma mass spectrometry (ICP-MS) or inductively coupled plasma optical emission spectroscopy (ICP-OES), with occasional utilization of X-ray fluorescence analysis (XRF) in the absence of total acid digestion.

Extraction solutions (e.g., ultrapure water, weak or strong ligand solutions), extraction methodologies (batch versus flow-through), and extraction durations varied among the referenced studies (Sholkovitz et al., 2012; Baker and Croot, 2010; Clough et al., 2020; Perron et al., 2020b). In this study, Fe extracted by ultrapure water and ammonium acetate buffer were uniformly classified as d-Fe, with the same approach applied for Al. Most aerosol samples from East Asia and the Pacific were extracted using ultrapure water, whereas a subset of Atlantic samples underwent extraction using ammonium acetate buffer at pH 4.7. Despite prior reports indicating that ammonium acetate extraction yields approximately 1.4 times greater Fe concentrations than ultrapure water (Perron et al., 2020b), no correction factor was applied in the present analysis.

2.2 Enrichment factor of Fe

To evaluate the sources of T-Fe in aerosol particles (*i.e.*, mineral Fe or anthro-Fe), the enrichment factor of Fe ($EF_{T\text{-}Fe}$) in aerosol particles is calculated by the following equation:

$$EF_{T-Fe} = \frac{(T-Fe/T-Al)_{aerosol}}{(T-Fe/T-Al)_{upper\ continental\ crust}} \quad \text{(Eq. 1)}$$

where $(T\text{-}Fe/T\text{-}Al)_{aerosol\ or\ upper\ continental\ crust}$ are mass ratio of T-Fe relative to T-Al ratio in aerosol particles and the average upper continental crust (UCC), respectively. Considering that T-Fe/T-Al ratio of the UCC varies among literatures, the $EF_{T\text{-}Fe}$ for all aerosol particles were recalculated. In this study, the mean T-Fe/T-Al ratio of 0.52 ± 0.12 in five studies was employed with the consideration of variability of the T-Fe/T-Al ratio in the upper continental crust (Turekian, 1961; Taylor, 1964; Taylor and McLennan, 1995; Wedepohl, 1995; Rudnick and Gao, 2003). While $EF_{T\text{-}Fe}$ greater than 10 is generally used to indicate a significant contribution from anthro-Fe (T-Fe/T-Al > 5.18), this study employed a lower threshold of 2.0 (T-Fe/T-Al: 1.04). This decision was made because even after accounting for the T-Fe/T-Al ratio and twice its standard deviation in source samples of Asian dust, Saharan dust, and other mineral dust, a statistically significant difference remained compared to twice the T-Fe/T-Al ratio of upper continental crust (Liu et al., 2022).

2.3 Data compilation of total and dissolved Fe and Al concentrations

2.3.1. Principle for a diagram between the $EF_{T\text{-}Fe}$ and [d-Fe]/[d-Al] ratio

The [d-Fe]/[d-Al] ratio and $EF_{T\text{-}Fe}$ in aerosol particles vary depending on emission sources and the dissolution processes of aerosol Fe (Sakata et al., 2023). The dominant sources of T-Fe and d-Fe in aerosol particles can be categorized into five

https://doi.org/10.5194/egusphere-2026-1613
Preprint. Discussion started: 8 April 2026

groups (Figure 1). $EF_{T\text{-}Fe}$ (vertical axis) is elevated by the influence of T-Fe-rich anthropogenic aerosols, whereas [d-Fe]/[d-Al] (horizontal axis) fluctuates mainly due to mineral dust dissolution processes, including proton-promoted and ligand-promoted dissolutions, and the input of highly soluble anthro-Fe. Aerosol samples strongly influenced by mineral dust are predominantly plotted within areas (i) and (ii), both characterized by $EF_{T\text{-}Fe}$ below 2.0. These areas differ based on the dissolution mechanisms of mineral dust: proton-promoted dissolution in area (i), where [d-Fe]/[d-Al] ranges from 0.1 to 1.0, and ligand-promoted (e.g., oxalate) dissolution in area (ii), where [d-Fe]/[d-Al] exceeds 1.0. Aerosol particles plotted in areas (iii) and (iv) are influenced by anthro-Fe, indicated by $EF_{T\text{-}Fe}$ greater than 2.0, with the distinction between these areas being the solubility of the anthro-Fe. In area (iii), insoluble anthro-Fe is primarily thought to stem from sources like non-exhaust vehicle particles (e.g., brake pad wear) and steel slag, which exhibited high T-Fe/T-Al ratio compared to mineral dust. The Fe_{sol}% of these anthro-Fe (<0.01%) is markedly lower than that of fresh mineral dust (Fe_{sol}%: 0.1–1.0%) (Halle et al., 2013; Shupert et al., 2021; Cui et al., 2025). As a result, although anthro-Fe contributes to enhance T-Fe/T-Al ratio, it has little impact on [d-Fe]/[d-Al] ratio. Therefore, [d-Fe]/[d-Al] ratio of aerosol particles in area (iii) is similar to mineral dust. In contrast, the anthro-Fe in area (iv) is easily dissolved, leading to an increase in the [d-Fe]/[d-Al] ratio. The readily soluble anthro-Fe discussed here encompasses exhibiting high Fe_{sol}% at the time of emission, and the initially insoluble anthro-Fe plotted in area (iii) that subsequently increased its solubility through atmospheric chemical processing. Finally, aerosol particles in area (v) originate from aluminosilicate glasses primarily emitted during combustion processes, including coal burning and municipal solid waste incineration, and are characterized by a [d-Fe]/[d-Al] ratio below 0.10. Assuming a binary mixing between areas (i) and (iv) in Figure 1, the fractions of d-Fe derived from mineral dust ($F_{mineral\text{-}dFe}$) and anthro-Fe ($F_{anthro\text{-}dFe}$) in aerosol particles are estimated by the following equations:

$$F_{mineral-dFe} + F_{anthro-dFe} = 1 \qquad \text{(Eq.2)}$$

$$\left(\left[\frac{\text{d-Fe}}{\text{d-Al}}\right]\right)_{\text{aerosol}} = \left(\left[\frac{\text{d-Fe}}{\text{d-Al}}\right]\right)_{\text{mineral}} \times F_{mineral} + \left(\left[\frac{\text{d-Fe}}{\text{d-Al}}\right]\right)_{\text{anthro}} \times F_{anthro} \qquad \text{(Eq. 3)}$$

A key limitation of this approach is the selection of appropriate representative [d-Fe]/[d-Al] for mineral dust and anthro-Fe. Representative [d-Fe]/[d-Al] ratios of mineral dust in East Asian/North Pacific and Atlantic aerosols were determined utilizing the values derived from Asian dust (= 0.24 ± 0.20, Duvall et al., 2008) and Saharan dust (= 0.11 ± 0.06, Desboeufs et al., 2001, 2024; Shi et al., 2011a). The mean [d-Fe]/[d-Al] ratio of fine aerosol particles collected in East Asia exceeding 1.5 was adopted as the representative [d-Fe]/[d-Al] ratio for anthro-Fe, yielding a value of 2.67 ± 1.88 (Sakata et al., 2023).

https://doi.org/10.5194/egusphere-2026-1613
Preprint. Discussion started: 8 April 2026

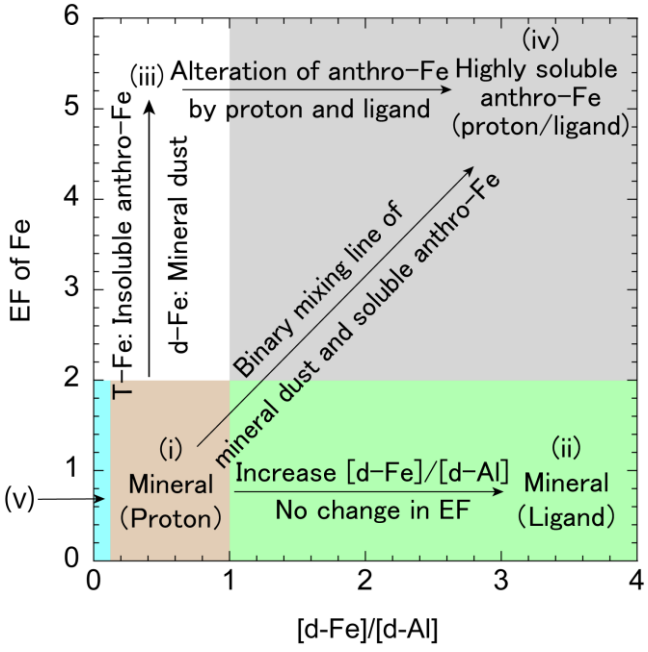

Figure 1. Relationships of emission sources of T-Fe and d-Fe with [d-Fe]/[d-Al] ratio and $EF_{T\text{-}Fe}$. This figure was partially modified from Sakata et al. (2025).

2.4 Principle for a diagram between the $EF_{T\text{-}Fe}$ and [d-Fe]/[d-Al] ratio

The Fe_{sol}% and Al_{sol}% were calculated by the following equations:

$$Fe_{sol}\% = \left(\frac{d-Fe}{T-Fe}\right)_{aerosol} \times 100 \qquad \text{(Eq. 4)}$$

$$Al_{sol}\% = \left(\frac{d-Al}{T-Al}\right)_{aerosol} \times 100 \qquad \text{(Eq. 5)}$$

In this study, Fe_{sol}% of mineral dust and anthropogenic aerosol (mineral-Fe_{sol}% and anthro-Fe_{sol}%, respectively) were evaluated separately. Mineral-Fe and anthro-Fe concentrations were determined using the following equations:

$$\text{Mineral Fe (ng m}^{-3}) = \text{Total Al} \times \left(\frac{T-Fe}{T-Al}\right)_{aerosol} \qquad \text{(Eq. 6)}$$

$$\text{Anthro Fe (ng m}^{-3}) = \text{Total Fe} - \text{Mineral Fe} \qquad \text{(Eq. 7)}$$

The d-Fe concentrations dissolved from mineral dust and anthro-Fe (mineral-dFe and anthro-dFe, respectively) were calculated by multiplying the d-Fe concentration by $F_{mineral}$ and F_{anthro}, respectively.

$$\text{Mineral dFe} = \text{dFe} \times F_{mineral-dFe} \qquad \text{(Eq. 8)}$$

$$\text{Anthro dFe} = \text{dFe} \times F_{anthro-dFe} \qquad \text{(Eq. 9)}$$

Finally, mineral-Fe_{sol}% and anthro-Fe_{sol}% were calculated using the same equation as Eq. 4.

https://doi.org/10.5194/egusphere-2026-1613
Preprint. Discussion started: 8 April 2026

3. Results and Discussion

3.1 Overview of global dataset

This compiled dataset integrates aerosol samples collected in East Asia with marine aerosol samples observed over the North and South Pacific, and Atlantic for which T-Fe, d-Fe, T-Al, and d-Al concentrations were all available. In total, the dataset includes 1,096 samples (East Asia: 428; North Pacific: 233; South Pacific: 91; Atlantic: 361), comprising TSP from all four regions and size-resolved coarse aerosol particles and fine aerosol particles from East Asia and the North Pacific where such measurements were available. Table 1 summarizes, for TSP in each region and basin, the dominant sources of T-Fe and d-Fe, as well as T-Fe concentration, d-Fe concentration, Fe_{sol}%, and $F_{anthro\text{-}dFe}$. Across the full dataset, T-Fe concentrations ranged from <0.1 to 14166.7 ng m^{-3} (mean: 278.1 ± 860.7 ng m^{-3}; median: 33.3 ng m^{-3}). High-T-Fe samples occurred mainly in East Asia, whereas samples from the North Pacific and South Pacific were concentrated in the low-T-Fe range; Atlantic samples showed an intermediate distribution (Table 1). d-Fe concentrations ranged from <0.1 to 212.7 ng m^{-3}, with the highest value observed in the Atlantic (Table 1). Although East Asian aerosols showed the highest mean d-Fe concentrations, the contrast with marine aerosols was much smaller than that for T-Fe, suggesting that d-Fe concentrations in marine aerosols cannot be explained solely by the transport flux of Fe-bearing aerosols from continental source regions.

Fe_{sol}%, which strongly affects d-Fe concentrations, showed a wide range from 0.01% to 99.95% (mean: 9.76 ± 15.2%; median: 4.57%). Mean Fe_{sol}% was lowest in East Asia and higher in the North Pacific, reflecting the strong influence of East Asian outflow. By comparison, Fe_{sol}% in the South Pacific and Atlantic was lower than in the North Pacific, suggesting that these regions are less strongly affected by processes that enhance Fe_{sol}%. As in previous studies, Fe_{sol}% increased as T-Fe concentration decreased in all regions (Figure 2a; Sholkovitz et al., 2012; Mahowald et al., 2018). This inverse relationship was observed commonly over both land and ocean, indicating that it is a globally shared characteristic (Figure 2a). Previous studies suggest that this relationship mainly reflects (1) preferential removal of coarse mineral dust with low solubility relative to fine anthro-Fe with higher solubility, which increases the relative importance of anthro-Fe as aerosol concentrations decrease, and (2) increased Fe_{sol}% through chemical processing during atmospheric transport (Mahowald et al., 2018). The sources of d-Fe in aerosols from each region and basin were evaluated using the [d-Fe]/[d-Al]-EF diagram. Many samples had T-Fe/T-Al ratios less than 2.0 and [d-Fe]/[d-Al] ratios less than 1.0, suggesting that T-Fe was derived mainly from mineral dust and that d-Fe was produced primarily through proton-promoted dissolution of those particles. Moreover, mean $F_{anthro\text{-}dFe}$ was less than 10% in all regions and basins, indicating that mineral dust-derived d-Fe is globally important for Fe supply to the ocean.

https://doi.org/10.5194/egusphere-2026-1613
Preprint. Discussion started: 8 April 2026

Table 1 Basin-scale summary of aerosol Fe (T-Fe and d-Fe ranges), Fe_{sol}%, and $F_{anthro\text{-}dFe}$ in East Asian and marine TSPs.

Area	**T-Fe source(s)**	**d-Fe source(s)**	**T-Fe range (ng m^{-3})**	**d-Fe range (ng m^{-3})**	**Fe_{sol}% (%)**	**$F_{anthro\text{-}dFe}$ (%)**
East Asia	TSP and coarse: Mineral dust Fine aerosol: Mineral dust + anthro-Fe	TSP and coarse: Fe dissolution from mineral dust Fine aerosols: Fe dissolution from mineral dust and antro-Fe emitted as insoluble Fe	Range: 15.6-14166.7 Mean: 1101.3 ± 1861.7	Range: 0.6-98.0 Mean: 12.6 ± 27.0	range: 0.1–17.5% Mean: 3.5 ± 3.2	7.9 ± 10.3
N. Pacific	Asian outflow of mineral dust	Fe dissolution from mineral dust: Fe_{sol}% in coarse aerosols was enhanced by chemical alteration in the marine atmosphere	Range: 0.2–764.5 Mean: 50.0 ± 104.4	Range: <0.1–45.9 Mean: 4.5 ± 7.3	Range: 0.4–74.2 Mean: 13.9 ± 14.4	Range: 6.1 ± 10.4 (max 73.7)
Atlantic	Saharan dust	episodic anthro-Fe supply from shipping Fe dissolution from mineral dust: cloud processing in high alitude Anthro-Fe mostly insoluble	Range: 0.2–5650.0 Mean: 387.2 ± 922.9	Range: <0.1–212.7 Mean: 6.9 ± 23.4	Range: 0.1–50.8 Mean: 6.2 ± 6.8	Range: 5.1 ± 9.7

https://doi.org/10.5194/egusphere-2026-1613
Preprint. Discussion started: 8 April 2026

Table 1 Basin-scale summary of aerosol Fe (T-Fe and d-Fe ranges), Fe_{sol}%, and $F_{anthro\text{-}dFe}$ in East Asian and marine TSPs.

Area	T-Fe source(s)	d-Fe source(s)	T-Fe range (ng m^{-3})	d-Fe range (ng m^{-3})	Fe_{sol}% (%)	$F_{anthro\text{-}dFe}$ (%)
S. Pacific	Mineral dust and volcanic influence near Heard Island	Coastal Australia aerosols affected by anthro emissions acidified aerosols. Volcanic influence near Heard Island	Range: 0.1–129.8 Mean: 17.6 ± 25.3	Range: <0.1–8.3 Mean: 1.0 ± 1.6	Range: <0.1–100 Mean: 8.5 ± 12.5 (excluding outlier: range: <0.1–41.9; Mean: 7.3 ± 6.4)	Up to 20% near Australia. Apparent high values near Heard Island are driven by volcanic ash (not anthro-Fe).

References. East Asia: Duvall et al., 2008; Kurisu et al., 2019; Hsieh et al., 2023; Sakata et al., 2023, 2025; Seo and Kim, 2023. The North Pacific: Buck et al., 2006, 2013; Marsay et al., 2022; Sakata et al., 2022; Kurisu et al., 2024. The Atlantic Ocean: Baker et al., 2006a, 2006b, 2013, 2020; Buck et al., 2010a, 2010b; Chance et al., 2015. The South Pacific: Buck et al., 2013, 2019; Sakata et al., 2022; Perron et al., 2020a, 2021.

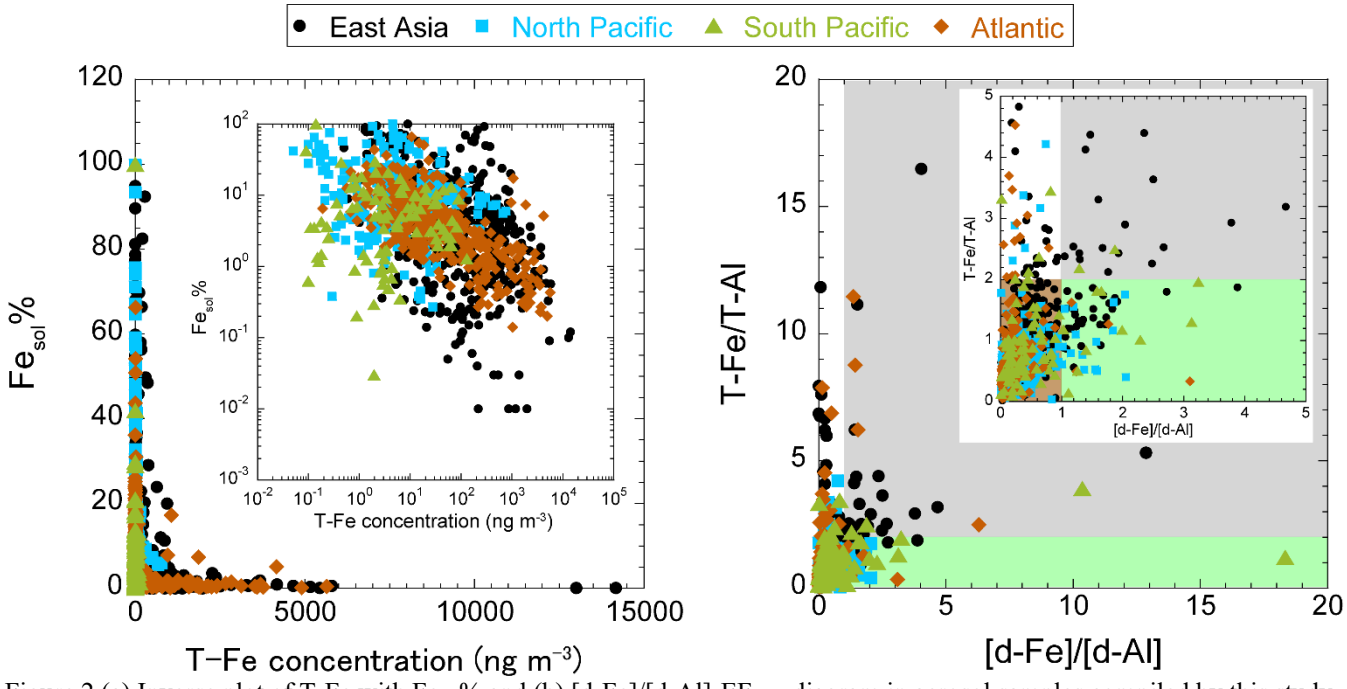

Figure 2 (a) Inverse plot of T-Fe with Fe_{sol}% and (b) [d-Fe]/[d-Al]-$EF_{T\text{-}Fe}$ diagram in aerosol samples compiled by this study.

https://doi.org/10.5194/egusphere-2026-1613
Preprint. Discussion started: 8 April 2026

3.2 East Asian aerosols

3.2.1 Monthly trends of Fe and Al concentrations

Elevated T-Fe and T-Al concentrations were primarily observed from March to May (Figure 3a), consistent with the seasonal trend of Asian dust transport from the Gobi and Taklamakan Deserts, which peaks in spring (Uematsu et al., 1983; Zhu et al., 2020; Kawai et al., 2021). T-Fe concentrations correlated strongly with T-Al concentrations in TSP samples (Figure S1a), and the mean $EF_{T\text{-}Fe}$ (1.6 ± 1.6; monthly mean: 1.2–1.9) was below 2.0.

The d-Fe and d-Al concentrations in TSP ranged from 0.6 to 98 ng m^{-3} and from 1 to 101 ng m^{-3}, respectively (Figure S1b). d-Fe concentrations were positively correlated with d-Al concentrations, suggesting that the two dissolved metals are influenced by similar processes (Figure S1b). Both d-Fe and d-Al concentrations tended to be higher in spring, consistent with the seasonal patterns of T-Fe and T-Al (Figure 3b). This indicated that the atmospheric loading of mineral dust and anthropogenic aerosols was an important factor influencing d-Fe variability. However, no significant correlations were found between T-Fe and d-Fe, or between T-Al and d-Al (Figures S1c and S1d), indicating that total elemental loading alone cannot explain the variability in dissolved metal concentrations. In contrast to T-Fe and T-Al, fine aerosol particles exhibited higher mean concentrations of d-Fe and d-Al (15 ± 37 ng m^{-3} and 22 ± 61 ng m^{-3}, respectively) than coarse aerosol particles (0.8 ± 1.2 ng m^{-3} and 1.5 ± 1.9 ng m^{-3}, respectively). These findings highlighted the important role of fine aerosol particles in supplying Fe to surface seawater via atmospheric deposition.

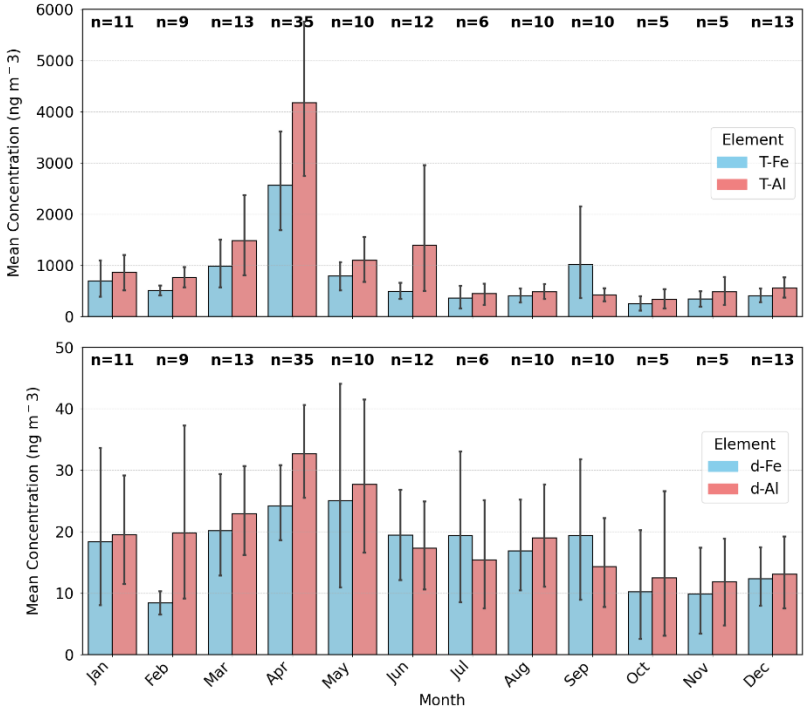

Figure 3. Monthly mean concentrations of (a) T-Fe and T-Al and (b) d-Fe and d-Al in East Asian TSP.

https://doi.org/10.5194/egusphere-2026-1613
Preprint. Discussion started: 8 April 2026

3.2.2 Factors controlling Fe_{sol}% of East Asian TSP

The annual mean Fe_{sol}% in East Asian TSP was 3.5 ± 3.2% (range: 0.1–17.5%), with higher values generally observed in summer (Figure 4a). Anthro-Fe likely contributed to the seasonal variation of Fe_{sol}% because $F_{anthro\text{-}dFe}$ also increased during summer. However, the annual mean $F_{anthro\text{-}dFe}$ in TSP was still limited to 7.9 ± 10.3%. Consistently, most East Asian TSP samples fell within regions (i) and (iii), indicating that T-Fe was derived mainly from mineral dust and insoluble anthro-Fe, whereas d-Fe was supplied primarily through proton-promoted dissolution of mineral dust rather than anthro-Fe (Figure 3a).

To investigate the mechanism underlying the inverse relationship between Fe_{sol}% and T-Fe concentration, we examined how mineral-Fe_{sol}% and anthro-Fe_{sol}% varied with their respective Fe concentrations. If this inverse relationship were governed solely by mixing between mineral dust with low Fe_{sol}% and highly soluble anthro-Fe, neither mineral-F_{esol}% nor anthro-Fe_{sol}% would be expected to depend on concentration. In contrast, both increased as Fe concentration decreased. These results indicate that the inverse relationship between Fe_{sol}% and T-Fe in East Asian TSP cannot be explained by simple source mixing alone, but instead reflects enhanced Fe dissolution of both mineral dust and anthro-Fe during chemical processing in atmospheric transport. Consistent with this interpretation, Japanese TSP collected during the Asian outflow season showed substantially higher solubility than Chinese and Korean TSP: the mean bulk Fe_{sol}% was 4.9 ± 3.6% in Japanese TSP, compared with 2.5 ± 2.5% in Chinese and Korean TSP. The same tendency was observed for mineral-Fe_{sol}% (6.6 ± 3.7% vs. 3.2 ± 4.1%) and anthro-Fe_{sol}% (3.1 ± 4.6% vs. 0.6 ± 1.1%). Together, these results support progressive solubilization of both mineral-Fe and anthro-Fe during transport from the East Asian continent.

Anthro-Fe in TSP could be further divided into two groups. One group exhibited lower Fesol% than mineral dust, whereas the other overlapped with mineral dust over a similar Fe concentration range. The boundary between these groups was defined as the lower 5th percentile limit of the power-law relationship between mineral-Fe concentration and mineral-Fe_{sol}%. The former group showed anthro-Fe_{sol}% values below 1% (mean: 0.3 ± 0.2%), with some high-concentration samples exhibiting extremely low solubility of <0.1%. This characteristic is consistent with non-combustion anthro-Fe, including brake-pad debris, tire-wear debris, and steel slags derived from road dust (Halle et al., 2013; Shupert et al., 2021; Cui et al., 2025). By contrast, the latter group had a mean anthro-Fe_{sol}% of 4.0 ± 5.7%, exceeding the mean mineral-Fe_{sol}% in East Asian TSP (2.4 ± 4.1%), which is consistent with the generally higher solubility expected for anthro-Fe derived from high-temperature combustion. Notably, even in high-anthro-Fe samples strongly influenced by fresh aerosol particles, anthro-Fe_{sol}% remained mostly around 1%. This suggests that these particles were not emitted in a highly soluble form, but instead became solubilized from an initially low-solubility state through chemical processing during atmospheric transport (Sholkovitz et al., 2009; Ito et al., 2021).

https://doi.org/10.5194/egusphere-2026-1613
Preprint. Discussion started: 8 April 2026

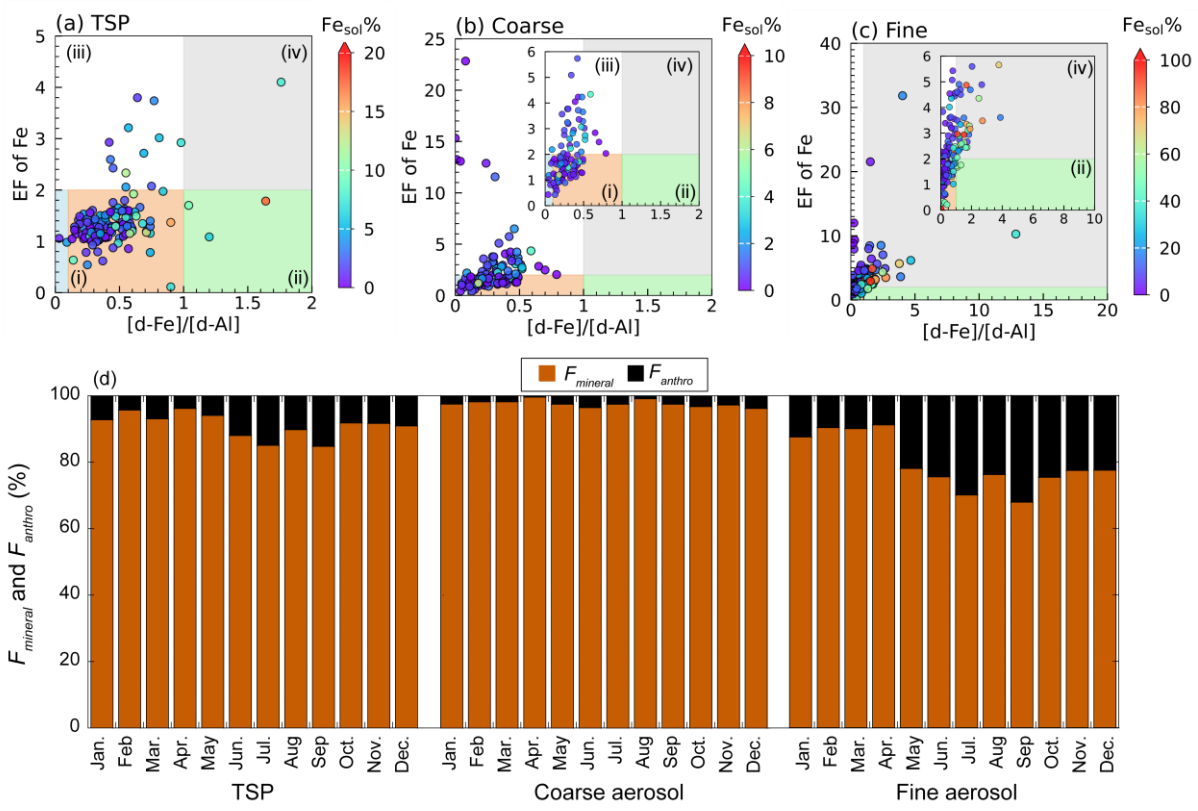

Figure 4. Diagrams between [d-Fe]/[d-Al] and $EF_{T\text{-}Fe}$ in (a) TSPs, (b) coarse aerosol particles and (c) fine aerosol particles and their magnified figures. (d) Monthly trends of $F_{mineral}$ and $F_{anthro\text{-}dFe}$ in TSP, coarse and fine aerosol particles.

255

3.2.3 Factors controlling Fe_{sol}% of East Asian coarse aerosol particles

The mean Fe_{sol}% in coarse aerosol particles was 1.0 ± 1.1%, and Fe_{sol}% was higher in summer. As well as TSPs, coarse aerosol particles were mainly plotted in area (i) and (iii), indicating that T-Fe in East Asina TSPs was mainly originated from mineral dust and insoluble anthro-Fe, and d-Fe was derived from proton-promoted dissolutions of mineral
260 dust (Figure 4a). The contribution of anthro-Fe to d-Fe in coarse aerosol particles was consistently low throughout the year, averaging only 2.4 ± 3.9% (Figure 5b).

Even in coarse aerosol particles, mineral-Fe_{sol}% increased as mineral-Fe concentration decreased (Figure 5b). Because there is little need to assume multiple initial Fe_{sol}% endmembers for mineral dust, this inverse correlation is interpreted as having been formed not by simple mixing, but by a combination of chemical processing during transport and depositional
265 removal. Indeed, the mean Fe_{sol}% of mineral dust in coarse aerosol particles was 2.3 ± 2.9%, slightly exceeding the range reported for fresh mineral dust (Duvall et al., 2008; Shi et al., 2011a; Desboeufs et al., 2001). However, mineral dust in coarse aerosol particles mainly exists as crystalline aluminosilicates and contains relatively high proportions of alkaline

https://doi.org/10.5194/egusphere-2026-1613
Preprint. Discussion started: 8 April 2026

minerals such as calcite ($CaCO_3$), making it less susceptible to strong acidification than fine aerosol particles. Acidification of Fe-bearing aluminosilicates is generally considered to proceed only after the buffering capacity of $CaCO_3$ has been consumed, yet $CaCO_3$ is known to remain even in coarse particles transported from the Gobi and Taklamakan to Japan (Meskhidze et al., 2005; Fairlie et al., 2010; Takahashi et al., 2009; Miyamoto et al., 2020). Therefore, substantial solubilization by aerosol acidification is unlikely in coarse aerosol particles, and the slight increase in observed Fe_{sol}% is likely attributable to partial transformation of Fe in chlorite and biotite into ferrihydrite and Fe(II, III)-sulfates (Takahashi et al., 2011; Sakata et al., 2025).

By contrast, the Fe_{sol}% of coarse aerosol particles (1.0 ± 1.1%) was lower than mineral-Fe_{sol}% (2.3 ± 2.9%), suggesting a contribution from low-solubility anthro-Fe. In fact, in Figure 4e, most anthro-Fe in coarse aerosol particles was distributed below the boundary line separating combusted and non-combusted anthro-Fe, with a mean anthro-Fe_{sol}% of 0.1 ± 0.2%, and an extremely low value of 0.05 ± 0.05% for the lower group. These particles are thought to correspond mainly to non-combustion anthro-Fe, such as resuspended non-exhaust vehicle particles and slag derived from steel-industry storage areas (Harrison et al., 2012; Kajino et al., 2020; Kurisu et al., 2019, 2026). Because this Fe mainly exists as Fe oxides and is less soluble than Fe in aluminosilicates under weakly acidic to neutral conditions, its contribution to d-Fe in coarse aerosol particles is likely small (Journet et al., 2008; Halle et al., 2013; Shupert et al., 2021; Cui et al., 2025).

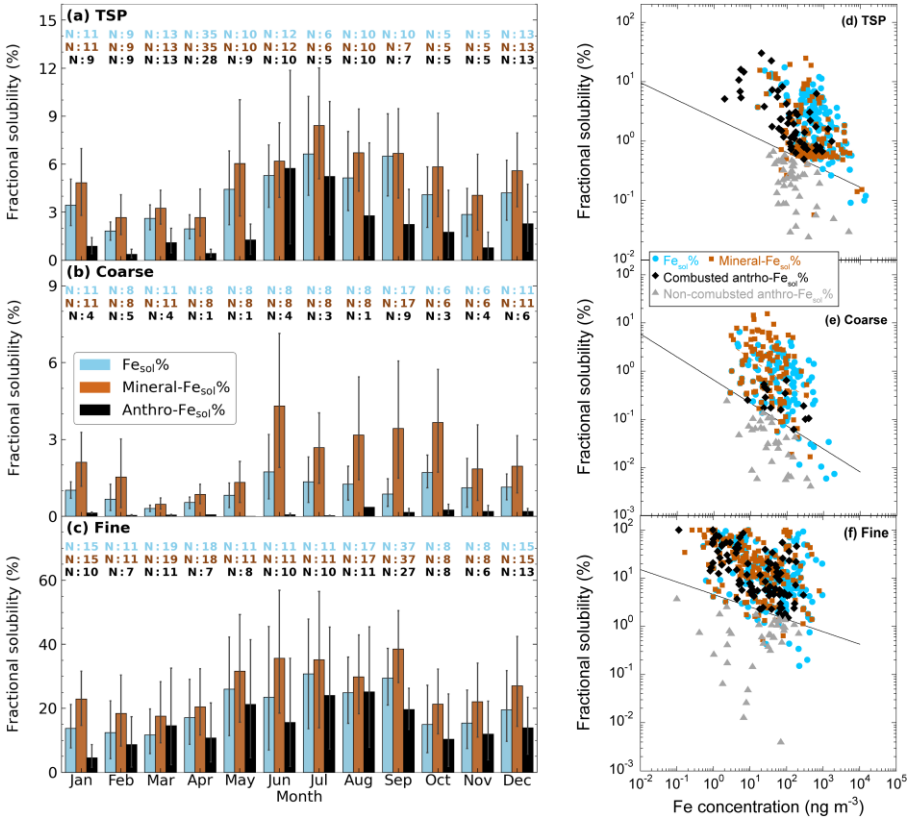

https://doi.org/10.5194/egusphere-2026-1613
Preprint. Discussion started: 8 April 2026

Figure 5. Monthly trends of Fe_{sol}%, mineral-Fe_{sol}%, and anthro-Fe_{sol}% in East Asia for (a) TSP, (b) coarse aerosol particles, and (c) fine aerosol particles. The red and black lines indicate the anthro-Fe_{sol}% enhancement associated with non-combustion-derived and combustion-derived anthro-Fe, respectively. Scatter plots of Fe concentration versus Fe_{sol}% for (d) TSP, (e) coarse aerosol particles, and (f) fine aerosol particles. The solid black lines in panels (d–f) denote the boundary separating non-combusted and combusted anthro-Fe.

3.2.4 Factors controlling Fe_{sol}% of East Asian fine aerosol particles

The annual mean bulk Fe_{sol}% in fine aerosol particles was 21.1 ± 23.6%, approximately one order of magnitude higher than that in coarse aerosol particles (1.0 ± 1.1%) (Figure 4b, c). In fine aerosol particles, both mineral-Fe_{sol}% (mean: 27.9 ± 28.0%) and anthro-Fe_{sol}% (mean: 16.0 ± 22.3%) exceeded 10%, indicating that both mineral dust and anthro-Fe contributed substantially to d-Fe. On average, 21.0 ± 26.3% of d-Fe in fine aerosol particles was derived from anthro-Fe.

Both mineral-Fe_{sol}% and anthro-Fe_{sol}% increased with decreasing their Fe concentrations in fine aerosol particles, providing clear evidence for solubilization during atmospheric transport (Figure 4f). This likely reflects the large specific surface area of fine aerosol particles and their greater susceptibility to reactions with acidic species and organic ligands. Among these processes, aerosol acidification is particularly important, because the pH of fine aerosol particles is typically more than one unit lower than that of coarse aerosol particles, which retain $CaCO_3$ (Guo et al., 2018; Pye et al., 2020). Consistent with this interpretation, single-particle analysis has identified sulfate coatings on both mineral dust and anthro-Fe in fine aerosol particles, and Fe(III)-sulfate has been detected in TSP and fine aerosol particles in Japan (Sullivan et al., 2007; Li et al., 2017; Zhu et al., 2022; Takahashi et al., 2013; Sakata et al., 2025). Moreover, Fe(III)-sulfate forms under highly acidic conditions (pH < 3.0), and $CaCO_3$ is absent from fine aerosol particles in Japan, suggesting that acidification in poorly buffered fine aerosol particles strongly promoted Fe dissolution (Meskhidze et al., 2005; Fairlie et al., 2010; Miyamoto et al., 2020; Sakata et al., 2022). Seasonal patterns also support this interpretation: in both coarse and fine aerosol particles, mineral-Fe_{sol}% and anthro-Fe_{sol}% were elevated in summer, consistent with lower aerosol pH and higher [nss-SO_4^{2-}]/[T-Fe] ratios during that season (Tao and Murphy, 2019b; Pye et al., 2020; Song and Osada, 2020; Sakata et al., 2025). Taken together, these results indicate that acidification is the dominant factor controlling the solubilization of Fe-containing particles in fine aerosol particles.

In contrast to coarse aerosol particles, anthro-Fe in fine aerosol particles was predominantly distributed above the boundary separating combusted and non-combusted anthro-Fe (Figure 4f). The group above the boundary showed a high mean anthro-Fe_{sol}% of 22.2 ± 24.0%, consistent with anthro-Fe derived from high-temperature combustion (Kurisu et al., 2021). Nevertheless, samples with anthro-Fe_{sol}% higher than 30% were not common even in the high-anthro-Fe concentration range, suggesting that anthro-Fe from solid-fuel combustion and high-temperature industrial processes, such as coal combustion and steel production, contributed more strongly than anthro-Fe from liquid-fuel combustion, such as heavy oil and gasoline combustion (Sedwick et al., 2007; Schroth et al., 2009; Oakes et al., 2012; Ito et al., 2021). By contrast, the

https://doi.org/10.5194/egusphere-2026-1613
Preprint. Discussion started: 8 April 2026

group below the boundary frequently showed anthro-Fe_{sol}% values of <0.1%, with a mean of 0.9 ± 0.8%, indicating the influence of non-combustion anthro-Fe, such as NEV particles, as also inferred for coarse aerosol particles (Kajino et al., 2020; Sakata et al., 2025). Because the maximum anthro-Fe_{sol}% in this group was only 3.7%, it was likely composed of Fe species that are intrinsically resistant to atmospheric solubilization. These results suggest that combustion-derived and non-combustion-derived anthro-Fe differ markedly in atmospheric reactivity.

3.3 The North Pacific Ocean

3.3.1 Monthly and spatial trend of T-Feand d-Fe concentration

T-Fe and T-Al concentrations in North Pacific TSPs ranged from 0.2 to 764.5 ng m^{-3} and 0.4 to 1320.7 ng m^{-3}, respectively. T-Fe was strongly correlated with T-Al, and the slope of the regression line was comparable to the T-Fe/T-Al ratio characteristic of mineral dust (Figure S2a). This suggests that T-Fe in North Pacific TSPs was primarily derived from mineral dust, consistent with the near-unity mean $EF_{T\text{-}Fe}$ value (1.3 ± 1.2). Concentrations of d-Fe and d-Al ranged from 0 to 45.9 ng m^{-3} and 0.1 to 70.8 ng m^{-3}, respectively, with d-Fe showing a strong correlation with d-Al (Figure S2b). The mean [d-Fe]/[d-Al] ratio of 0.39 ± 0.29 aligns with values for mineral dust subjected to proton-promoted dissolution. These results indicate that both T-Fe and d-Fe in North Pacific TSPs largely originated from mineral dust.

Distinct from East Asian aerosols, North Pacific aerosols exhibited strong correlations between d-Fe and T-Fe concentrations, as well as between d-Al and T-Al concentrations (Figure S2c). This suggests that the amount of d-Fe supplied to the North Pacific is primarily controlled by the total transport flux of T-Fe-containing aerosols. Shipboard observations revealed that T-Fe and d-Fe concentrations in the marine boundary layer decreased with increasing distance from East Asia (Figures 5a and 5b), indicating the deposition of T-Fe and d-Fe-containing particles from the atmosphere to the ocean during transport. Furthermore, the highest T-Fe and d-Fe concentrations were observed in spring, coinciding with the period of mineral dust transport from the Gobi and Taklamakan deserts (Figures 6a and 6b).

This spatial and seasonal pattern is broadly consistent with satellite-derived dust aerosol optical depth (DAOD), a proxy for the atmospheric column abundance of mineral dust (Song et al., 2021). Satellite observations also show enhanced surface seawater chlorophyll a following dust events over the North Pacific (Luo et al., 2020; Yoon et al., 2022), suggesting that continental mineral dust is an important source of d-Fe supporting biological primary production in this region. These results highlight the importance of understanding both the seasonality of Fe emission sources and the processes controlling Fe_{sol}% in North Pacific aerosols.

https://doi.org/10.5194/egusphere-2026-1613
Preprint. Discussion started: 8 April 2026

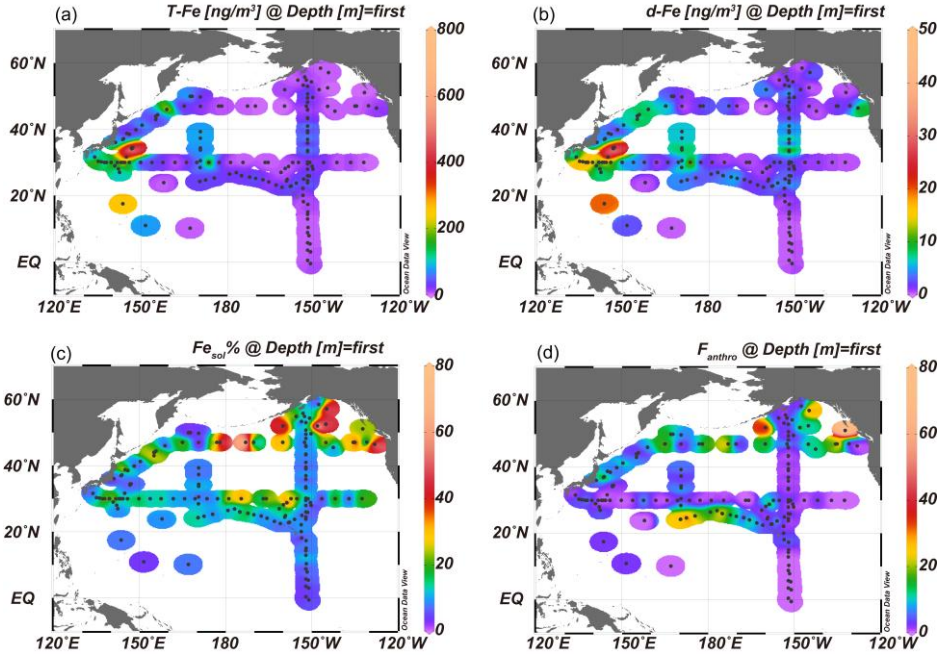

Figure 6. Spatial distributions of (a) T-Fe concentration, (b) d-Fe concentration, (c) Fe_{sol}%, and (d) F_{anthro} in the North Pacific TSP samples.

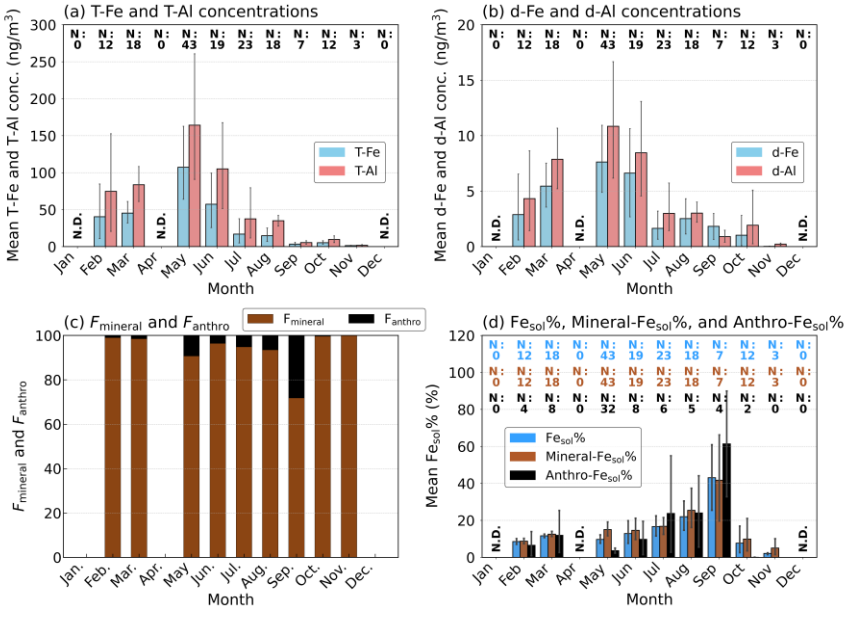

Figure 7. Monthly trends of (a) T-Fe concentration, (b) d-Fe concentration, (c) Fe_{sol}%, and (d) $F_{anthro\text{-}dFe}$ in the North Pacific TSP samples.

https://doi.org/10.5194/egusphere-2026-1613
Preprint. Discussion started: 8 April 2026

3.3.2 The impact of anthro-Fe on Fe_{sol}% in the North Pacific aerosols

Figure S3a shows the relationship between [d-Fe]/[d-Al] and $EF_{T\text{-}Fe}$ in North Pacific TSP samples. Consistent with the mineral dust dominance described above, most samples were distributed within the proton-promoted dissolution regime for mineral dust (area (ii) in Figure S3a). Nevertheless, several samples exhibited $EF_{T\text{-}Fe}$ values greater than 2.0, indicating that anthro-Fe contributed to T-Fe in North Pacific aerosols. Moreover, 67 of the 155 samples had a detectable anthro-Fe contribution to d-Fe ($F_{anthro\text{-}dFe} > 0$). Among these, 37 samples had $F_{anthro\text{-}dFe}$ values above 10% (maximum: 73.7%), indicating that anthro-Fe was a non-negligible contributor to d-Fe in at least some North Pacific aerosols.

Following the same approach used for East Asia, anthro-Fe was further classified into combusted anthro-Fe (33 samples) and non-combusted anthro-Fe (34 samples) according to whether anthro-Fe_{sol}% overlapped with mineral-Fe_{sol}% at similar Fe concentrations (Figure 7a). Most samples below the boundary were collected from February to May, when East Asian outflow is strong, suggesting a substantial influence of continental anthropogenic emissions. Their mean anthro-Fe_{sol}% was 1.0 ± 0.8%, and although anthro-Fe_{sol}% increased slightly with decreasing concentration, the maximum value was only 2.7%. These particles occurred in both coarse aerosol particles and fine aerosol particles, and their persistently low solubility resembled that of non-exhaust vehicle particles such as brake-pad debris (Figures 7b and 7c). Accordingly, non-combusted anthro-Fe, including NEV particles, likely remains largely insoluble even after long-range transport over the marine atmosphere and probably contributes little to d-Fe supply in the North Pacific.

By contrast, samples above the boundary showed a high mean anthro-Fe_{sol}% of 23.2 ± 26.5%. These particles occurred predominantly in fine aerosol particles, with only minor contributions in the coarse fraction (Figures 7b and 7c), suggesting a primary association with high-temperature combustion sources. During February to May, when East Asian outflow is strongest, anthro-Fe_{sol}% in this group tended to be lower than the overall mean, consistent with a substantial contribution from East Asia-derived solid-fuel combustion, for which anthro-Fe_{sol}% at emission is not necessarily high. In contrast, during summer, particularly in September when the influence of Asian outflow weakened, combusted anthro-Fe often showed anthro-Fe_{sol}% values higher than the mean for samples above the boundary. This pattern likely contributed to the enhanced influence of anthro-Fe in TSP during this period (Figure 6c). One plausible seasonal source is heavy-oil combustion from ship traffic along the major shipping route linking East Asia and North America. A previous modeling study estimated that approximately 40% of d-Fe in North Pacific aerosols was derived from ship emissions (Ito, 2013), and ship emissions are known to contain highly soluble Fe at emission (Fe_{sol}% > 30%; Schroth et al., 2009; Oakes et al., 2011). Thus, ship-related anthro-Fe may efficiently enhance Fe_{sol}% in summer. However, because d-Fe concentrations in North Pacific aerosols were lower in summer than in other seasons (Figures 6b and 6d), the annual contribution of ship-related anthro-Fe to total d-Fe deposition is likely limited.

https://doi.org/10.5194/egusphere-2026-1613
Preprint. Discussion started: 8 April 2026

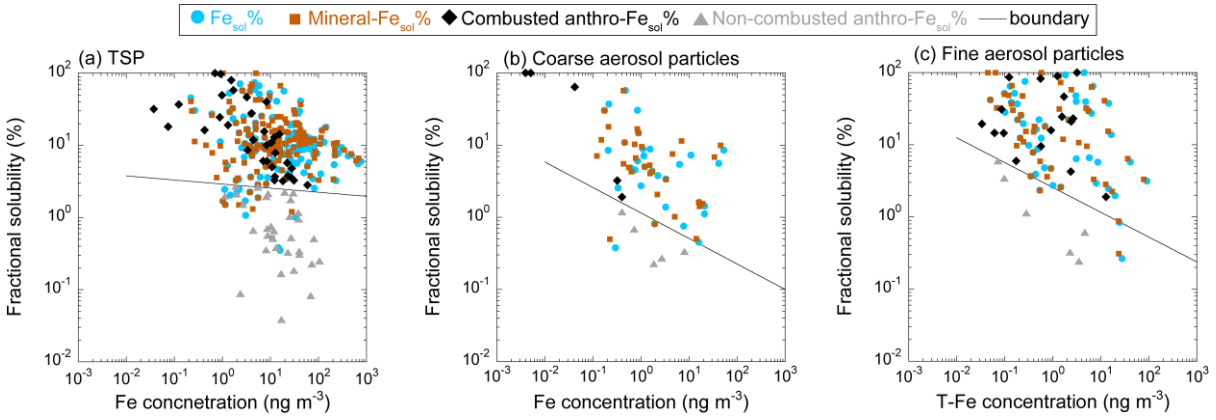

Figure 8. Inverse relationships between T-Fe, mineral-Fe, and anthro-Fe and their respective Fe solubilities in (a) TSP, (b) coarse aerosol particles, and (c) fine aerosol particles collected in the North Pacific. Black solid lines show the boundary separating non-combusted and combusted anthro-Fe

3.3.3 The impact of chemical alterations on Fe_{sol}% in the North Pacific aerosols

The mean Fe_{sol}%, mineral-Fe_{sol}%, and anthro-Fe_{sol}% of North Pacific TSP were higher than those of East Asian aerosols during winter and spring, when Asian outflow is strongest (Table 2). This indicates that East Asian outflow aerosols undergo further chemical alteration during transport over the North Pacific. Comparison of coarse aerosol particles and fine aerosol particles showed that both mineral-Fe_{sol}% and anthro-Fe_{sol}% increased in coarse aerosol particles during transport from Japan to the North Pacific, whereas values in fine aerosol particles remained largely unchanged. A similar pattern was observed for Al_{sol}%, an indicator of mineral dust alteration, which was also higher in coarse aerosol particles from the North Pacific than in those from East Asia (Table 2). These results suggest that chemical aging continues in coarse aerosol particles during marine transport, whereas Fe dissolution in fine aerosol particles is already close to completion by the time the aerosols reach Japan. Given that fine aerosol particles generally exhibit higher reactivity than coarse aerosol particles because of their larger specific surface area, the marked increase in Fe_{sol}% and Al_{sol}% specifically in coarse aerosol particles is particularly notable and requires additional explanation.

The similar Fe_{sol}% values of fine aerosol particles in East Asia and the North Pacific suggest that most Fe dissolution in this size fraction has already occurred during transport within East Asia (Table 2). This interpretation is consistent with kinetic models showing that Fe dissolution proceeds rapidly at first and then approaches a plateau, as well as with previous applications of such models indicating that Fe dissolution in fine aerosol particles over the Sea of Japan and the North Pacific is already close to the plateau stage (Shi et al., 2011b, 2015; Maters et al., 2016; Sakata et al., 2022, 2025). Thus, further transport over the marine atmosphere would not be expected to produce a large additional increase in Fe_{sol}%. At the same time, cloud processing should promote ferrihydrite precipitation if only inorganic Fe speciation is considered, implying

https://doi.org/10.5194/egusphere-2026-1613
Preprint. Discussion started: 8 April 2026

that some mechanism must stabilize dissolved Fe during marine transport. A likely mechanism is complexation with organic ligands. Wu et al. (2023) showed that the Fe_{sol}% of fine aerosol particles collected on Matsu Island remained high for 30 days in seawater amended with deferoxamine, whereas it dropped to below 1% without deferoxamine. In addition, Fe(III)-HULIS has been detected in fine aerosol particles over the North Pacific (Sakata et al., 2022; Kurisu et al., 2024). Because such complexes remain soluble over a wide pH range, complexation with marine organic matter likely helps preserve d-Fe during cloud processing and may also facilitate transfer of soluble Fe to the ocean.

Table 2. Annual means of Fe_{sol}%, mineral-Fe_{sol}%, and anthro-Fe_{sol}% in TSP, coarse aerosol particles, and fine aerosol particles collected in East Asia and the North Pacific (%). The parentheses show the mean Fe_{sol}% in aerosol particles collected from winter to spring (December to May).

		TSP		Coarse aerosol particles		Fine aerosol particles	
		East Asia	North Pacific	East Asia	North Pacific	East Asia	North Pacific
Fe_{sol}%	Annual Sample No.	3.5 ± 3.2 *N*: 139	13.9 ± 14.4 *N*: 155	1.0 ± 1.0 *N*: 110	9.2 ± 12.8 *N*: 31	21.0 ± 23.6 *N*: 181	24.3 ± 24.9 *N*: 47
	Winter-spring Sample No.	2.8 ± 2.7 *N*: 91	10.5 ± 6.5 *N*: 73	0.8 ± 0.7 *N*: 57	*6.0 ± 4.6*[a] *N*: 10	16.3 ± 19.3 *N*: 86	13.1 ± 16.4 N: 20
Mineral-Fe_{sol}%	Annual Sample No.	4.7 ± 4.5 *N*: 137	16.3 ± 16.6 *N*: 155	2.3 ± 2.9 *N*: 110	8.9 ± 11.0 *N*: 31	27.9 ± 28.0 *N*: 181	28.5 ± 28.7 *N*: 47
	Winter-spring Sample No.	3.8 ± 4.2 *N*: 91	13.4 ± 10.7 *N*: 73	2.8 ± 2.7 *N*: 57	*4.8 ± 10.0*[a] *N*: 10	22.5 ± 23.4 *N*: 86	15.2 ± 18.1 N: 20
Anthro-Fe_{sol}%	Annual Sample No.	1.7 ± 4.1 *N*: 91	12.1 ± 21.8 *N*: 69	0.1 ± 0.2 *N*: 45	*11.3 ± 30.2*[a] *N*: 10	16.0 ± 22.4 *N*: 56	26.2 ± 32.0 N: 23
	Winter-spring Sample	1.0 ± 2.0 *N*: 81	5.4 ± 8.9 *N*: 44	0.1 ± 0.1 *N*: 21	*0.9 ± 3.0*[a] *N*: 3	12.3 ± 20.1 *N*: 181	*17.4 ± 27.5*[a] *N*: 8

https://doi.org/10.5194/egusphere-2026-1613
Preprint. Discussion started: 8 April 2026

	No.						
	Annual	2.9 ± 2.4	10.5 ± 9.3	2.2 ± 2.5	11.8 ± 16.2	16.3 ± 15.0	20.2 ± 17.0
	Sample No.	*N*: 139	*N*: 155	*N*: 110	*N*: 31	*N*: 181	*N*: 47
Al_{sol}%	Winter-spring	2.5 ± 2.6	8.5 ± 5.1	1.5 ± 1.8	*11.4 ± 15.3*[a]	13.2 ± 11.7	13.5 ± 13.1
	Sample No.	*N*: 91	*N*: 73	N: 57	*N*: 10	*N*: 86	*N*: 20

[a]The italicized values are based on a very small number of samples (N ≤ 10); therefore, these values should be regarded as indicative.

By contrast, aerosol acidification is unlikely to be the main reason for elevated Fe_{sol}% in coarse aerosol particles over the North Pacific, because previous modeling studies have suggested that calcite buffering remains effective during transport, and charge-balance calculations likewise indicate that coarse aerosol particles over the North Pacific do not contain sufficient acidity to exhaust the buffering capacity of calcite (Meskhidze et al., 2005; Ito and Feng, 2010; Fairlie et al., 2010; Sakata et al., 2022). Instead, ligand-promoted dissolution appears more plausible. Several coarse aerosol samples were plotted in area (ii) of the [d-Fe]/[d-Al]–$EF_{T\text{-}Fe}$ diagram, where d-Fe is interpreted to be supplied mainly by ligand-promoted dissolution of mineral dust, and these samples showed a high mean Fe_{sol}% of 39.9 ± 22.4%. Although the number of such samples was limited, this pattern suggests that organic ligands in the marine atmosphere can substantially enhance Fe dissolution in coarse aerosol particles during transport. This interpretation is supported by experimental results showing that the Fe_{sol}% of coarse aerosol particles from Matsu Island increased from a few percent to about 10% when exposed to a simulated marine organic ligand under seawater pH conditions (Wu et al., 2023). These results indicate that Fe in coarse aerosol particles retains the capacity for further dissolution by organic ligands, although more direct observational evidence is still needed to constrain the importance of this process over the North Pacific.

3.4 The Atlantic aerosols

3.4.1 Spatial and monthly trend of T-Fe and d-Fe concentrations

The T-Fe and T-Al concentrations in the Atlantic TSPs ranged from 0.2 to 5650.0 ng m^{-3} and from 0.8 to 7485.0 ng m^{-3}, respectively. The high concentration of T-Fe was mainly found in the coastal region of the Saharan Desert extending to 20–30°W between 10–20°N (Figure 8a). T-Fe concentration in the Atlantic TSPs was correlated with T-Al concentration and the slope of its regression line (0.60) closely matched T-Fe/T-Al ratio of mineral dust. Indeed, the mean value of $EF_{T\text{-}Fe}$ was 1.5 ± 1.7, indicating that mineral dust is the most dominant source of T-Fe in the Atlantic TSPs.

https://doi.org/10.5194/egusphere-2026-1613
Preprint. Discussion started: 8 April 2026

Concentrations of d-Fe and d-Al ranged from <0.1 to 212.7 ng m^{-3} and from <0.1 to 336.6 ng m^{-3}, respectively. The d-Fe concentration in Atlantic TSPs was correlated with d-Al concentration, indicating that these dissolved metal concentrations were controlled by similar processes (Figure S4b). However, unlike T-Fe, the highest d-Fe concentrations were not observed in the coastal region of the Sahara Desert, but mainly in the region between 20–30°W and 10–20°N (Figure 8b). This result suggests that, unlike North Pacific aerosols, d-Fe and d-Al concentrations in Atlantic aerosols were not controlled simply by mineral dust loading, as also reflected by the weak correlations of d-Fe with T-Fe and d-Al with T-Al (Figures S4c and S4d). The relatively low d-Fe concentrations in the coastal Saharan region are therefore attributable to the low Fe_{sol}% of freshly emitted mineral dust. Some Atlantic aerosols were also plotted in area (iii), whereas almost none fell in area (iv) (Figure S3b), implying that anthro-Fe in Atlantic aerosols was predominantly present in an insoluble form and contributed little to d-Fe.

https://doi.org/10.5194/egusphere-2026-1613
Preprint. Discussion started: 8 April 2026

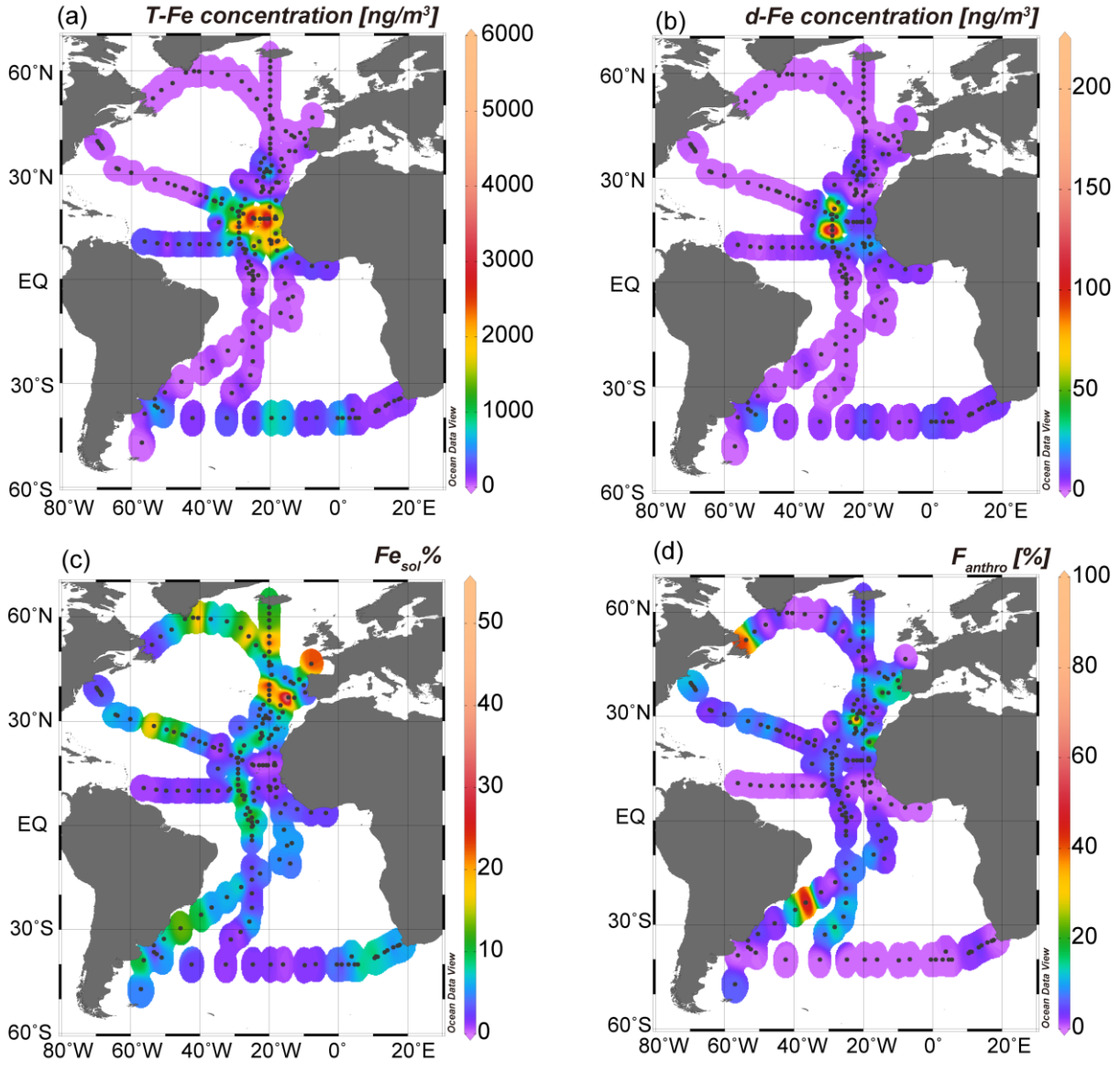

Figure 9. Spatial distributions of (a) T-Fe concentration, (b) d-Fe concentration, (c) Fe_{sol}%, and (d) $F_{anthro\text{-}dFe}$ in the Atlantic aerosols.

Unfortunately, Atlantic TSP samples collected from February to April are not available in this dataset. However, shipboard observations showed that T-Fe and T-Al concentrations were clearly higher in winter than in summer (Figure 9a), consistent with previous ground-based observational studies at Cape Verde, located offshore of the Sahara Desert (Carpenter et al., 2010; Fomba et al., 2013; Patey et al., 2015). In contrast, satellite observations of DAOD indicate a summer peak, which is also consistent with the seasonal variability of dust deposition fluxes recorded by sediment traps in seawater (Yu et al., 2019;

https://doi.org/10.5194/egusphere-2026-1613
Preprint. Discussion started: 8 April 2026

van der Does et al., 2021). This discrepancy is most likely explained by seasonal differences in the transport altitude of Saharan dust. During summer, the northward shift of the Intertropical Convergence Zone (ITCZ) leads to the convergence of moist air from the south and dry air from the north between 15°N and 22°N, forming the Saharan Air Layer (SAL), which lifts mineral dust to altitudes of 5–7 km and transports it westward over the Atlantic Ocean (Adams et al., 2012; Muhs et al., 2013). In winter to spring, mineral dust is transported mainly in the lower troposphere and is therefore readily captured by shipboard and ground-based observations. As a result, DAOD and wet deposition to the ocean are enhanced in summer, whereas the signal in near-surface observations becomes weaker (van der Does et al., 2021). Therefore, in the Atlantic Ocean, particularly in regions offshore of the Sahara, it may be difficult to comprehensively understand aerosol Fe supply processes based solely on shipboard and ground-based observations.

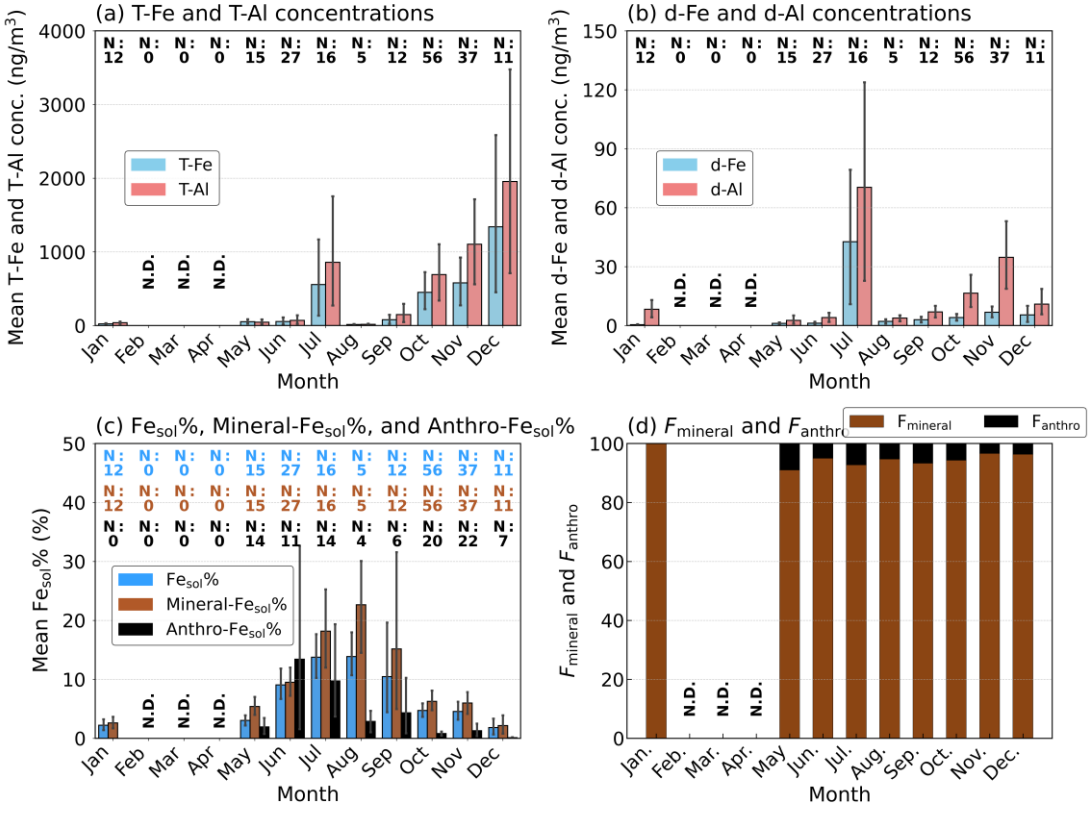

Figure 10. Monthly variations of (a) T-Fe and T-Al concentrations, (b) d-Fe and d-Al concentrations, (c) Fe_{sol}%, mineral-Fe_{sol}%, and anthro-Fe_{sol}%, and (d) $F_{mineral}$ and $F_{anthro\text{-}dFe}$ in the Atlantic aerosols.

https://doi.org/10.5194/egusphere-2026-1613
Preprint. Discussion started: 8 April 2026

3.4.2 The impact of anthro-Fe on Fe_{sol}%

The annual mean Fe_{sol}% of Atlantic TSPs was 6.2 ± 6.8% (range: 0.1–50.8%), and Fe_{sol}% tended to be higher in summer (Figure 9c). High Fe_{sol}% values (>10%) were predominantly observed in the coastal regions of Europe and North America (Figure 8c). Previous studies have reported negative Fe isotope signatures attributable to combustion-derived anthro-Fe in these regions (Conway et al., 2019). However, comparison of Figures 8c and 8d shows that the locations of high Fe_{sol}% do not necessarily coincide with those of elevated $F_{anthro\text{-}dFe}$, suggesting that combustion-derived anthro-Fe is not a primary driver of the spatial variability in Fe_{sol}% over the Atlantic.

This interpretation is further supported by the source apportionment results for anthro-Fe. Most anthro-Fe in Atlantic aerosol samples was distributed below the boundary line, with a mean anthro-Fe_{sol}% of 1.0 ± 1.7%. This indicates that anthro-Fe in Atlantic aerosols was dominated primarily by non-combustion-derived, low-solubility Fe. In contrast, relatively soluble combustion-derived anthro-Fe, represented by samples plotted above the boundary line, was rare, with a mean anthro-Fe_{sol}% of 14.5 ± 22.2%. A similar pattern was observed in both coarse and fine aerosol particles (Figures 10b and 10c). These results suggest that anthro-Fe contributed little to the direct increase in d-Fe or to the enhancement of bulk Fe_{sol}%. Therefore, the seasonal and spatial variability of Fe_{sol}% in Atlantic aerosols was more likely controlled by the aging state of mineral dust than by anthro-Fe input.

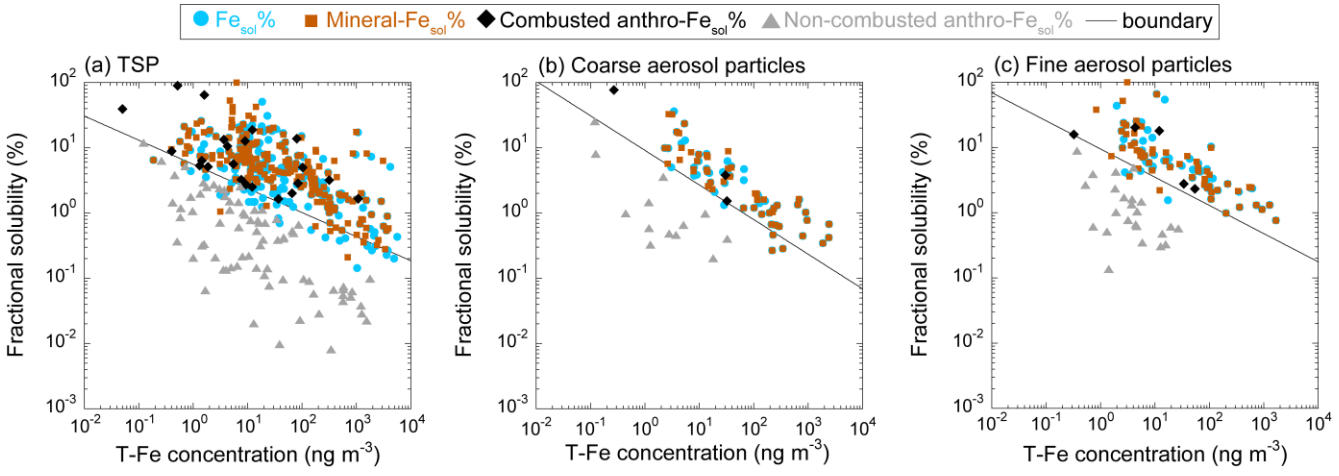

Figure 11. The inverse relationship of T-Fe, mineral-Fe, and anthro-Fe with their respective concentrations in (a) TSP, (b) coarse aerosol particles, and (c) fine aerosol particles collected in the Atlantic. The solid black lines show the boundary separating on-combusted and combusted anthro-Fe.

3.4.3 The impact of chemical alteration on Fe_{sol}%

The monthly average Fe_{sol}% of Atlantic aerosols tended to be higher in summer than in other seasons (Figure 9c). The same trend was found in the latitude band most affected by the Sahara Desert (Equator to 30°N). The East Asian region

https://doi.org/10.5194/egusphere-2026-1613
Preprint. Discussion started: 8 April 2026

shows comparable seasonal variability in Fe_{sol}% (Figure 4a–4c), which has been attributed primarily to the temperature dependence of aerosol pH. In contrast, the Sahara-affected latitude band experiences relatively minor annual temperature effects, suggesting that other factors contribute to the observed seasonal variability of Fe_{sol}%.

A likely explanation is the seasonal difference in the transport altitude and atmospheric processing of Saharan dust. In winter, mineral dust is transported mainly below 3 km. Because there are no heavily polluted regions between the Sahara Desert and the Atlantic Ocean, the dust is not strongly aged by atmospheric pollutants such as sulfate and nitrate (Fitzgerald et al., 2015). Furthermore, relatively low precipitation in winter likely suppresses wet deposition and chemical alteration in cloud water. Consequently, Atlantic aerosol samples collected near the surface in winter exhibited higher Fe concentrations but lower Fe_{sol}%. During summer, by contrast, mineral dust is predominantly transported above 3 km, where precipitation is higher. In particular, the increase in precipitation from August to October (Varela-Lopes and Molion, 2014) likely promotes the incorporation of mineral dust into cloud water, where aqueous-phase reactions driven by proton-promoted and ligand-promoted dissolution may enhance Fe_{sol}%. However, under the moderately acidic conditions of Atlantic cloud water (pH > 4.0; Shah et al., 2020), Fe dissolution is not expected to be as substantial as in more acidic regions, even in the presence of organic ligands (Bibi et al., 2011; Paris et al., 2011; Paris and Desboeufs, 2013; Bray et al., 2015). Observations using aerosol time-of-flight mass spectrometry also confirmed that mineral dust over the Atlantic undergoes chemical alteration by oxalate in cloud water (Fitzgerald et al., 2015). Thus, summer cloud-water processing likely enhances Fe_{sol}% in Atlantic aerosols, but not to the extent observed in the North Pacific, where aerosol acidity is often much stronger, as reflected by the lower mean Fe_{sol}% of Atlantic aerosols (5.9%) than of North Pacific aerosols (15.1%).

3.5 The South Pacific Ocean

The T-Fe and T-Al concentrations in South Pacific TSPs ranged from 0.1 to 129.8 ng m^{-3} and 0.2 to 207.2 ng m^{-3}, respectively, with the highest values observed in coastal regions (Figure 11a). T-Fe was strongly correlated with T-Al (slope = 0.92), and the mean $EF_{T\text{-}Fe}$ was 1.9 ± 1.4 (range: 0.1–7.6). The $EF_{T\text{-}Fe}$ in the South Pacific TSPs was slightly higher than in North Pacific and Atlantic TSPs but still close to unity. $EF_{T\text{-}Fe}$ tended to be elevated in the marine area southeast of Australia, especially around Heard Island (Figure S5), likely reflecting the influence of volcanic bedrock on the island (Perron et al., 2021). Overall, however, T-Fe in South Pacific TSPs was derived mainly from mineral dust.

The concentrations of d-Fe and d-Al ranged from <0.1 to 8.3 ng m^{-3} and <0.1 to 12.6 ng m^{-3}, respectively, and showed a strong correlation (r = 0.77). Fe_{sol}% ranged from <0.1 to 100% (mean: 8.5 ± 12.5%); excluding one sample with Fe_{sol}% of 100%, the maximum was 41.9% and the mean was 7.3 ± 6.4%. The mean [d-Fe]/[d-Al] ratio in South Pacific TSPs was 0.73 ± 1.30, higher than those in North Pacific and Atlantic TSPs (0.39 ± 0.29 and 0.25 ± 0.48, respectively). High $F_{anthro\text{-}dFe}$ values, characterized by elevated [d-Fe]/[d-Al], were mainly detected near Heard Island, where $EF_{T\text{-}Fe}$ was also high (Figure S5). Given the basaltic volcanic rocks on Heard Island, this enrichment is more plausibly explained by volcanic source composition than by enhanced anthropogenic input (Perron et al., 2021).

https://doi.org/10.5194/egusphere-2026-1613
Preprint. Discussion started: 8 April 2026

TSP samples with Fe_{sol}% exceeding 10% were mainly observed along the Australian coast. Previous studies reported that elevated Fe_{sol}% on the southeastern coast reflects anthro-Fe from urban areas together with aerosol acidification driven by anthropogenic SO_2 and NOx (Perron et al., 2020a). Consistent with this interpretation, our [d-Fe]/[d-Al] analysis suggests that up to ~20% of d-Fe in this region was derived from anthro-Fe. In northern and northeastern Australia, high Fe_{sol}% has also been linked to biomass burning (Perron et al., 2020a). However, previous studies suggest that Fe associated with biomass burning mainly reflects resuspended dry soil rather than direct Fe emission (Andreae et al., 2001; Kurisu and Takahashi, 2019), and observations at Gun Point indicate that the elevated Fe_{sol}% is driven not by direct d-Fe emission but by chemical interactions between Fe and organic matter emitted during fires (Winton et al., 2016). Consistent with this, TSP samples from northeastern Australia showed [d-Fe]/[d-Al] ratios above 1.0 despite $EF_{T\text{-}Fe}$ values below 2.0 (Figure S3c), a pattern consistent with ligand-promoted dissolution of mineral dust. High $F_{anthro\text{-}dFe}$ values were also observed in southeastern Australia, where volcanic rocks with high T-Fe/T-Al ratios have been reported. This suggests that the elevated [d-Fe]/[d-Al] ratio in this region may likewise reflect source-composition effects rather than anthropogenic input, although further investigation is needed.

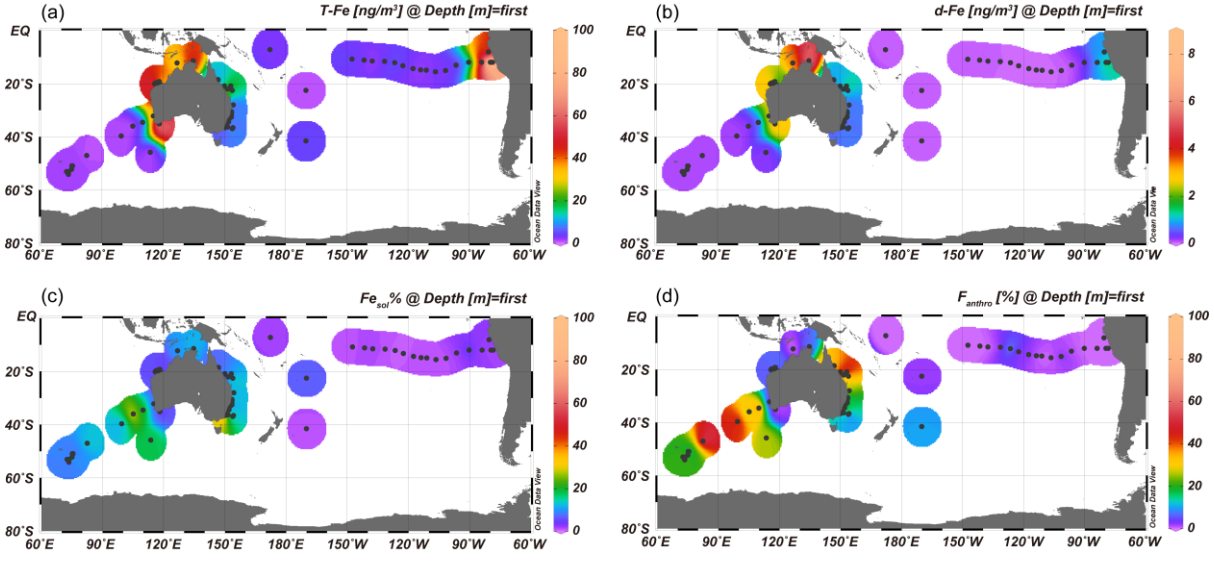

Figure 12. Spatial distribution of (a) Fe_{sol}% and (b) $F_{anthro\text{-}dFe}$ in the South Pacific aerosols. (c) inverse relationship between Fe concentration and its Fe_{sol}%.

4. Implications

This study estimated $F_{anthro\text{-}dFe}$ in marine aerosol particles based on the [d-Fe]/[d-Al] ratio. As a result, the contribution of anthro-Fe to d-Fe in the marine TSP samples was not large (North Pacific: 6.1 ± 10.4, Atlantic: 5.1 ± 9.7%). Although high $F_{anthro\text{-}dFe}$ was occasionally found in North Pacific TSPs influenced by ship emissions, $F_{anthro\text{-}dFe}$ in the pelagic region

https://doi.org/10.5194/egusphere-2026-1613
Preprint. Discussion started: 8 April 2026

was lower than coastal regions. Complementing our findings, Fe isotope analysis of d-Fe in marine aerosols consistently indicates large and small anthropogenic contributions to d-Fe in coastal and in the pelagic regions, respectively (Labatut et al., 2014; Conway et al., 2019; Kurisu et al., 2021, 2024). In contrast to these observational results, modeling studies showed the remarkable contribution of anthro-Fe to d-Fe ($F_{anthro\text{-}dFe}$ > 20%, Hamilton et al., 2019; Rathod et al., 2020, 2024; Ito et al., 2021; Ito and Miyakawa, 2023). This discrepancy of $F_{anthro\text{-}dFe}$ between models and observational data can partly be attributed to the lower dissolution rates of Fe in mineral dust adopted in the models compared to field measurements. In many models, the dissolution rate of mineral dust is often set to a maximum of around 10%. However, our results showed that mineral-Fe_{sol}% in fine aerosol particles were often higher than 10% (North Pacific: 28.5 ± 28.7%, Atlantic: 11.3 ± 16.7%). Given that fine aerosol particles displayed higher d-Fe concentrations compared to coarse aerosol particles, and that anthro-Fe is primarily found in fine aerosol particles, an underestimation of mineral-Fe_{sol}% in fine aerosol particles likely led to an overestimation of $F_{anthro\text{-}dFe}$.

To better understand the sources of d-Fe in marine aerosols and their chemical alteration processes, observational studies, focusing on the [d-Fe]/[d-Al] ratio and Fe isotope ratios, are essential. These studies help us grasp the factors influencing $F_{anthro\text{-}dFe}$, $F_{mineral\text{-}dFe}$, mineral-Fe_{sol}%, and anthro-Fe_{sol}% variability. While representative values for mineral dust are established for both [d-Fe]/[d-Al] and Fe isotope ratios, large uncertainties persist regarding representative values for anthro-Fe and the variability among different emission sources. Constructing a robust database of [d-Fe]/[d-Al] and Fe isotope ratios for individual anthropogenic emission sources (e.g., coal combustion, steel industry, biomass burning, and non-combusted anthro-Fe) is crucial because the representative values of [d-Fe]/[d-Al] and Fe isotope ratios for anthro-Fe affect the calculation results of $F_{mineral\text{-}dFe}$ and $F_{anthro\text{-}dFe}$.

Code and data availability

Data archiving is underway in Zenodo, and the dataset will be made publicly available via Zenodo upon acceptance (doi: 10.5281/zenodo.19186414).

Supplement link

The link to the supplement will be included by Copernicus, if applicable.

https://doi.org/10.5194/egusphere-2026-1613
Preprint. Discussion started: 8 April 2026

Author contributions

KS and YT designed this study. KS and MT compiled dataset using this study. KS developed the model and performed the simulations. KS prepared the manuscript with contributions from all co-authors.

Competing interests

The authors declare that they have no conflict of interest.

Acknowledgements

The International GEOTRACES program is possible in part thanks to the support from the U.S. National Science Foundation (Grant OCE-2140395) to the Scientific Committee on Oceanic Research (SCOR). This paper also contributes to the science plan of the Surface Ocean-Lower Atmosphere Study (SOLAS), which is partially supported by the U.S. National Science Foundation (Grant OCE-1840868) via the Scientific Committee on Oceanic Research (SCOR).

Review statement

The review statement will be added by Copernicus Publications listing the handling editor as well as all contributing referees according to their status anonymous or identified.

References

Adams, A. M., Prospero, J. M., Zhang, C.: CALIPSO-derived three-dimensional structure of aerosol over the Atlantic basin and adjacent continents, J. Clim., 25, 6862–6879, https://doi.org/10.1175/JCLI-D-11-00672.1, 2012.

Andreae, M. O., Fischer, A. H., Freitas, S. R., Grégoire, J. M., Hoor, H. P., Kormann, R., Krejci, R., Lange, L., Lelieveld, J., Lindinger, W., Longo, K., Peters, W., de Reus, M., Scheeren, B., Silva, M. A. F., Ström, J., van Velthoven, P. F. J., Williams, J.: Transport of biomass burning smoke to the upper troposphere by deep convection in the equatorial region, Geophys. Res. Lett., 28, 951–954, https://doi.org/10.1029/2000GL012391, 2001.

Baker, A. R., Adams, C., Bell, T. G., Jickells, T. D., Ganzeveld, L.: Estimation of atmospheric nutrient inputs to the Atlantic Ocean from 50°N to 50°S based on large-scale field sampling: Iron and other dust-associated elements, Global Biogeochem. Cycles, 27, 755–767, https://doi.org/10.1002/gbc.20062, 2013.

Baker, A. R., Croot, P. L.: Atmospheric and marine controls on aerosol iron solubility in seawater, Mar. Chem., 120, 4–13, https://doi.org/10.1016/j.marchem.2008.09.003, 2010.

Baker, A. R., French, M., Linge, K. L.: Trends in aerosol nutrient solubility along a west–east transect of the Saharan dust plume, Geophys. Res. Lett., 33, L07805, https://doi.org/10.1029/2005GL024764, 2006a.

Baker, A. R., Jickells, T. D., Witt, M., Linge, K. L.: Trends in the solubility of iron, aluminium, manganese and phosphorus in aerosol collected over the Atlantic Ocean, Mar. Chem., 98, 43–58, https://doi.org/10.1016/j.marchem.2005.06.004, 2006b.

https://doi.org/10.5194/egusphere-2026-1613
Preprint. Discussion started: 8 April 2026

Baker, A. R., Kanakidou, M., Nenes, A., Myriokefalitakis, S., Croot, P. L., Duce, R. A., Gao, Y., Guieu, C., Ito, A., Jickells, T. D., Mahowald, N. M., Middag, R., Perron, M. M. G., Sarin, M. M., Shelley, R., and Turner, D. R.: Changing atmospheric acidity as a modulator of nutrient deposition and ocean biogeochemistry, Sci. Adv., 7, eabd8800, https://doi.org/10.1126/sciadv.abd8800, 2021.

Baker, A. R., Li, M., Chance, R.: Trace metal fractional solubility in size-segregated aerosols from the tropical eastern Atlantic Ocean, Global Biogeochem. Cycles, 34, e2019GB006510, https://doi.org/10.1029/2019GB006510, 2020.

Bibi, I., Singh, B., Silvester, E.: Dissolution of illite in saline–acidic solutions at 25°C, Geochim. Cosmochim. Acta, 75, 3237–3249, https://doi.org/10.1016/j.gca.2011.03.022, 2011.

Boyd, P. W., Jickells, T., Law, C. S., Blain, S., Boyle, E. A., Buesseler, K. O.: Mesoscale iron enrichment experiments 1993–2005: Synthesis, and future directions, Science, 315, 612–617, https://doi.org/10.1126/science.1131669, 2007.

Bray, A. W., Oelkers, E. H., Bonneville, S., Wolff-Boenisch, D., Potts, N. J., Fones, G., Benning, L. G.: The effect of pH, grain size, and organic ligands on biotite weathering rates, Geochim. Cosmochim. Acta, 164, 127–145, https://doi.org/10.1016/j.gca.2015.04.048, 2015.

Buck, C. S., Landing, W. M., Resing, J. A.: Particle size and aerosol iron solubility: A high-resolution analysis of Atlantic aerosols, Mar. Chem., 120, 14–24, https://doi.org/10.1016/j.marchem.2008.11.002, 2010b.

Buck, C. S., Landing, W. M., Resing, J. A., Lebon, G. T.: Aerosol iron and aluminum solubility in the northwest Pacific Ocean: Results from the 2002 IOC cruise, Geochem. Geophys. Geosyst., 7, Q04M07, https://doi.org/10.1029/2005GC000977, 2006.

Buck, C. S., Landing, W. M., Resing, J. A., Measures, C. I.: The solubility and deposition of aerosol Fe and other trace elements in the North Atlantic Ocean: Observations from the A16N CLIVAR/CO2 repeat hydrography section, Mar. Chem., 120, 57–70, https://doi.org/10.1016/j.marchem.2008.08.003, 2010a.

Buck, C. S., Landing, W. M., Resing.: Pacific Ocean aerosols: Deposition and solubility of iron, aluminum, and other trace elements, Mar. Chem., 157, 117–130, https://doi.org/10.1016/j.marchem.2013.09.005, 2013.

Buck, C. S., Paytan, A.: Evaluation of commonly used filter substates for the measurement of aerosol trace element solubility, Limnol Oceanogr Methods, 10, 790–806, https://doi.org/10.4319/lom.2012.10.790, 2012.

Buck, C.S., Aguilar-Islas, A., Marsay, C., Kadko, D., Landing, W. M.: Trace element concentrations, elemental ratios, and enrichment factors observed in aerosol samples collected during the US GEOTRACES eastern Pacific Ocean transect (GP16), Chem. Geol., 511, 212–224, https://doi.org/10.1016/j.chemgeo.2019.01.002, 2019.

Carpenter, L. J., Fleming, Z. L., Read, K. A., Lee, J. D., Moller, S. J., Hopkins, J. R., Purvis, R. M., Lewis, A. C., Müller, K., Heinold, B., Herrmann, H., Fomba, K. W., van Pinxteren, D., Müller, C., Tegen, I., Wiedensohler, A., Müller, T., Niedermeier, N., Achterberg, E. P., Patey, M. D., Kozlova, E. A., Manning, A. J., and Wallace, D. W. R.: Seasonal characteristics of tropical marine boundary layer air measured at the Cape Verde Atmospheric Observatory, J. Atmos. Chem., 67, 87–140, https://doi.org/10.1007/s10874-011-9206-1, 2011.

Chance, R., Jickells, T. D., Baker, A. R.: Atmospheric trace metal concentrations, solubility and deposition fluxes in remote marine air over the south-east Atlantic, Mar. Chem., 177, 45–56, https://doi.org/10.1016/j.marchem.2015.06.028, 2015.

Charlson, R. J., Lovelock, J. E., Andreae, M. O., Warren, S. G.: Oceanic phytoplankton, atmospheric sulphur, cloud albedo and climate, Nature, 326, 655–661, https://doi.org/10.1038/326655a0, 1987.

Clough, R., Lohan, M. C., Ussher, S. J., Nimmo, M., Worsfold, P. J.: Uncertainty associated with the leaching of aerosol filters for the determination of metals in aerosol particulate matter using collision/reaction cell ICP-MS detection, Talanta, 208, 120377, https://doi.org/10.1016/j.talanta.2019.02.067, 2020.

Conway, T. M., Hamiliton, D. S., Shelley, R. U., Aguilar-Islas, A. M., Landing, W. M., Mahowald, N. M., John, S. G.: Tracing and constraining anthropogenic aerosol iron fluxes to the North Atlantic Ocean using iron isotopes, Nat. Commun., 10, 2628, https://doi.org/10.1038/s41467-019-10457-w, 2019.

Cui, W., Song, X., Su, Y., Chen, X., Wu, D., Li, Q.: Soluble iron in source-based anthropogenic $PM_{2.5}$ predominantly from steel industry and residential combustion in China, Geophys. Res. Lett., 52, e2025GL118603, https://doi.org/10.1029/2025GL118603, 2025.

https://doi.org/10.5194/egusphere-2026-1613
Preprint. Discussion started: 8 April 2026

Desboeufs, K. V., Losno, R., Colin, J. L.: Factors influencing aerosol solubility during cloud processes, Atmos. Environ., 35, 3529–3537, https://doi.org/10.1016/S1352-2310(00)00472-6, 2001.

Desboeufs, K., Formenti, P., Torres-Sánchez, R., Schepanski, K., Chaboureau, J.-P., Andersen, H., Cermak, J., Feuerstein, S., Laurent, B., Klopper, D., Namwoonde, A., Cazaunau, M., Chevaillier, S., Feron, A., Mirande-Bret, C., Triquet, S., and Piketh, S. J.: Fractional solubility of iron in mineral dust aerosols over coastal Namibia: a link to marine biogenic emissions?, Atmos. Chem. Phys., 24, 1525–1541, https://doi.org/10.5194/acp-24-1525-2024, 2024.

Duvall, R. M., Majestic, B. J., Shafer, M. M., Chuang, P. Y., Simoneit, B. R. T. Schauer, J. J.: The water-soluble fraction of carbon, sulfur, and crustal elements in Asian aerosols and Asian soils, Atmos. Environ., 42, 5872–5884, https://doi.org/10.1016/j.atmosenv.2008.03.028, 2008.

Fairlie, T. D., Jacob, D. J., Dibb, J. E., Alexander, B., Avery, M. A., van Deonklelaar, A., Zhang, L.: Impact of mineral dust on nitrate, sulfate, and ozone in transpacific Asian pollution plumes, Atmos. Chem. Phys., 10, 3999–4012, https://doi.org/10.5194/acp-10-3999-2010, 2010.

Fitzgerald, E., Ault, A. P., Zauscher, M. D., Mayol-Bracero, O. L., Prather, K. A.: Comparison of the mixing state of long-range transported Asian and African mineral dust, Atmos. Environ., 115, 19–25, https://doi.org/10.1016/j.atmosenv.2015.04.031, 2015.

Fomba, K. W., Müller, K., van Pinxteren, D., Herrmann, H.: Aerosol size-resolved trace metal composition in remote northern tropical Atlantic marine environment: case study Cape Verde islands, Atmos. Chem. Phys., 13, 4801–4814, https://doi.org/10.5194/acp-13-4801-2013, 2013.

Guo, H., Nenes, A., Weber, R. J.: The underappreciated role of nonvolatile cations in aerosol ammonium-sulfate molar ratios, Atmos. Chem. Phys., 18, 173407–17323, https://doi.org/10.5194/acp-18-17307-2018, 2018.

Guo, H., Sullivan, A. P., Campuzano-Jost, P., Schroder, J. C., Lopez-Hilfiker, F. D., Dibb, J. E., Jimenez, J. L., Thornton, J. A., Brown, S. S., Nenes, A., and Weber, R. J.: Fine particle pH and the partitioning of nitric acid during winter in the northeastern United States, J. Geophys. Res. Atmos., 121, 10355–10376, https://doi.org/10.1002/2016JD025311, 2016.

Halle, L. L., Palmqvist, A., Kampmann, K., Jensen, A., Hansen, T., Khan, F. R.: Tire wear particle and leachate exposures from a pristine and road-worn tire to Hyalella azteca: Comparison of chemical content and biological effects, Aquat Toxicol, 232, 105769, https://doi.org/10.1016/j.aquatox.2021.105769, 2021.

Hamilton, D. S., Scanza, R. A., Feng, Y., Guinness, J., Kok, J. F., Li, L., Liu, X., Rathod, S. D., Wan, J. S., Wu, M., and Mahowald, N. M.: Improved methodologies for Earth system modelling of atmospheric soluble iron and observation comparisons using the Mechanism of Intermediate complexity for Modelling Iron (MIMI v1.0), Geosci. Model Dev., 12, 3835–3862, https://doi.org/10.5194/gmd-12-3835-2019, 2019.

Harrison, R. M., Jones, A. M., Gietl, J., Yin, J., Green, D. C.: Estimation of the contributions of brake dust, tire wear, and resuspension to nonexhaust traffic particles derived from atmospheric measurements, Environ. Sci. Technol., 2012, 46, 6523–6529, https://doi.org/10.1021/es300894r, 2012.

Hsieh, C. C., You, C. F., Ho, T. Y.: The solubility and deposition flux of East Asian aerosol metals in the East China Sea: The effects of aeolian transport processes, Mar. Chem., 253, 104268, https://doi.org/10.1016/j.marchem.2023.104268, 2023.

Ito, A.: Global modeling study of potentially bioavailable iron input from shipboard aerosol sources to the ocean, Global Biogeochem. Cycles, 27, 1–10, https://doi.org/10.1029/2012GB004378, 2013.

Ito, A. Feng, Y.: Role of dust alkalinity in acid mobilization of iron, Atmos. Chem. Phys., 10, 9237–9250, https://doi.org/10.5194/acp-10-9237-2010, 2010.

Ito, A. and Miyakawa, T.: Aerosol iron from metal production as a secondary source of bioaccessible iron, Environ. Sci. Technol., 57, 4091–4100, https://doi.org/10.1021/acs.est.2c06472, 2023.

Ito, A., Myriokefalitakis, S., Kanakidou, M., Mahowald, N. M., Scanza, R. A., Hamilton, D. S., Baker, A. R., Jickells, T. D., Sarin, M. M., Bikkina, S., Gao, Y., Shelley, R. U., Buck, C. S., Landing, W. M., Bowie, A. R., Perron, M. M. G., Guieu, C., Meskhidze, N., Johnson, M. S., Feng, Y., Kok, J. F., Nenes, A., and Duce, R. A.: Pyrogenic iron: The missing link to high iron solubility in aerosols, Sci. Adv., 5, eaau7671, https://doi.org/10.1126/sciadv.aau7671, 2019.

https://doi.org/10.5194/egusphere-2026-1613
Preprint. Discussion started: 8 April 2026

Ito, A., Ye, Y., Baldo, C., Shi, Z.: Ocean fertilization by pyrogenic aerosol iron, npj Clim. Atmos. Sci., 4, 30, https://doi.org/10.1038/s41612-021-00185-8, 2021.

Jickells, T. D., An, Z. S., Andersen, K. K., Baker, A. R., Bergametti, G., Brooks, N., Cao, J. J., Boyd, P. W., Duce, R. A., Hunter, K. A., Kawahata, H., Kubilay, N., LaRoche, J., Liss, P. S., Mahowald, N. M., Prospero, J. M., Ridgwell, A. J., Tegen, I., and Torres, R.: Global iron connections between desert dust, ocean biogeochemistry, and climate, Science, 308, 67–71, https://doi.org/10.1126/science.1105959, 2005.

Jin, X., Frenzel, G. H., Doney, S. C., McWilliams, J. C.: The impact of atmospheric CO_2 of iron fertilization induced changes in the ocean's biological pump, Biogeosci., 5, 385–406, https://doi.org/10.5194/bg-5-385-2008, 2008.

Journet, E., Desboeufs, K. V., Caquineau, S., Colin, J. L.: Mineralogy as a critical factor of dust iron solubility, Geophys. Res. Lett., 35, L07805, https://doi.org/10.1029/2007GL031589, 2008.

Kajino, M., Hagino, H., Fujitani, Y., Morikawa, T., Fukui, T., Onishi, K., Okuda, T., Kajikawa, T., Igarashi, Y.: Modeling transition metals in East Asia and Japan and its emission sources, GeoHealth, 4, e2020GH000259, https://doi.org/10.1029/2020GH000259, 2020.

Kanakidou, M., Myriokefalitakis, S., Tsigaridis, K.: Aerosols in atmospheric chemistry and biogeochemical cycles of nutrients, Environ. Res. Lett., 13, 063004, https://doi.org/10.1088/1748-9326/aabcdb, 2018.

Kawai, K., Matsui, H., Tobo, Y.: High potential of Asian dust to act as ice nucleating particles in mixed-phase clouds simulated with a global aerosol-climate model, J. Geophys. Res. Atmos., 126, e2020JD034263, https://doi.org/10.1029/2020JD034263, 2021.

Krishnamurthy, A., Moore, J. K., Mahowald, N., Luo, C., Doney, S., Linday, K., Zender, C. S.: Impacts of increasing anthropogenic soluble iron and nitrogen deposition on ocean biogeochemistry, Global Biogeochem. Cycles, 23, GB3016, https://doi.org/10.1029/2008GB003440, 2009.

Kurisu, M., Adachi, K., Sakata, K., Takahashi, Y.: Stable isotope ratios of combustion iron produced by evaporation in a steel plant, ACS Earth Space Chem.. 3, 588–598, https://doi.org/10.1021/acsearthspacechem.8b00171, 2019.

Kurisu, M., Sakata, K., Nishioka, J., Obata, H., Conway, T. M., Hunt, H. R., Sieber, M., Suzuki, K., Kashiwabara, T., Kubo, S., Takada, M., and Takahashi, Y.: Source and fate of atmospheric iron supplied to the subarctic North Pacific traced by stable iron isotope ratios, Geochim. Cosmochim. Acta, 378, 168–185, https://doi.org/10.1016/j.gca.2024.06.009, 2024.

Kurisu, M., Sakata, K., Uematsu, M., Ito, A., Takahashi, Y.: Contribution of combustion Fe in marine aerosols over the northwestern Pacific estimated by Fe stable isotope ratio, Atmos. Chem. Phys., 21, 16027–16050, https://doi.org/10.5194/acp-21-16027-2021, 2021.

Kurisu, M., Takahashi, Y.: Testing iron stable isotope ratios as signature of biomass burning, Atmos., 10, 76, https://doi.org/10.3390/atmos10020076, 2019.

Kurisu, M., Zhu, C., Miyakawa, T., Ito, A., Suzuki, K., Kashiwabara, T.: Identification of anthropogenic Fe originated from East Asia using Fe stable isotope ratios of aerosols collected on Fukue Island, Atmos. Environ., 373, 121893, https://doi.org/10.1016/j.atmosenv.2026.121893, 2026.

Kurokawa, J., and Ohara, T.: Long-term historical trends in air pollutant emissions in Asia: Regional emission inventory in Asia (REAS) version 3, Atmos. Chem. Phys., 20, 12761–12793, https://doi.org/10.5194/acp-20-12761-2020, 2020.

Labatut, M., Lacan, F., Pradoux, C., Chmeleff, J., Radic, A., Murray, J. W., Poitrasson, F., Johansen, A. M., and Thil, F.: Iron sources and dissolved-particulate interactions in the seawater of the Western Equatorial Pacific, iron isotope perspectives, Global Biogeochem. Cycles, 28, 1044–1065, https://doi.org/10.1002/2014GB004928, 2014.

Li, T., Wang, Y., Li, W.J., Chen, J. M., Wang, T., Wang, W. X.: Concentrations and solubility of trace elements in fine particles at a mountain site, southern China: regional sources and cloud processing, Atmos. Chem. Phys., 15, 8987–9002, https://doi.org/10.5194/acp-15-8987-2015, 2015.

Li, W., Xu, L., Liu, X., Zhang, J., Lin, Y., Yao, X., Gao, H., Zhang, D., Chen, J., Wang, W., Harrison, R., Shao, L., Fu, P., Nenes, A., and Shi, Z.: Air pollution–aerosol interactions produce more bioavailable iron for ocean ecosystems, Sci. Adv., 3, e1601749, https://doi.org/10.1126/sciadv.1601749, 2017.

https://doi.org/10.5194/egusphere-2026-1613
Preprint. Discussion started: 8 April 2026

Liu, X., Turner, J. R.., Hand, J. L., Schichtel, B. A., Martin, R. V.: A global-scale mineral dust equation, J. Geophys. Res. Atmos., 127, e2022JD036937, 2022.

Luo, C., Wang, W., Sheng, L., Zhou, Y., Hu, Z., Qu, W., Li, X., and Hai, S.: Influence of polluted dust on chlorophyll-a concentration and particulate organic carbon in the subarctic North Pacific Ocean based on satellite observation and the WRF-Chem simulation, Atmos. Res., 236, 104812, https://doi.org/10.1016/j.atmosres.2019.104812, 2020.

Ma, Q., Cai, S., Wang, S., Zhao, B., Martin, R. V., Brauer, M., Cohen, A., Jiang, J., Zhou, W., Hao, J., Frostad, J., Forouzanfar, M. H., and Burnett, R. T.: Impacts of coal burning on ambient PM2.5 pollution in China, Atmos. Chem. Phys., 17, 4477–4491, https://doi.org/10.5194/acp-17-4477-2017, 2017.

Mahowald, N. M., Engelstaedter, S., Luo, C., Sealy, A., Artaxo, P., Benitez-Nelson, C., Bonnet, S., Chen, Y., Chuang, P. Y., Cohen, D. D., Dulac, F., Herut, B., Johansen, A. M., Kubilay, N., Losno, R., Maenhaut, W., Paytan, A., Prospero, J. M., Shank, L. M., and Siefert, R. L.: Atmospheric iron deposition: Global distribution, variability and human perturbations, Ann. Rev. Mar. Sci., 1, 245–278, https://doi.org/10.1146/annurev.marine.010908.163727, 2009.

Mahowald, N. M., Hamilton, D. S., Mackey, K. R. M., Moore, J. K., Baker, A. R., Scanza, R. A. and Zhang, Y.: Aerosol trace metal leaching and impacts on marine microorganisms, Nat. Commun., 9, 1–15, https://doi.org/10.1038/s41467-018-04970-7, 2018.

Marsay, C. M., Kadko, D., Landing, W. M., Buck, C.: Bulk aerosol trace element concentrations and deposition fluxes during the U.S, GEOTRACES GP15 Pacific meridional transect, Global Biogeochem. Cycles, 36, e2021GB007122, https://doi.org/10.1029/2021GB007122, 2022.

Martin, J. H.: Glacial-interglacial CO_2 change: The iron hypothesis, Paleoceanography, 5, 1–13, https://doi.org/10.1029/PA005i001p00001, 1990.

Martin, J. H., Coale, K. H., Johnson, K. S., Fitzwater, S. E., Gordon, R. M., Tanner, S. J., Hunter, C. N., Elrod, V. A., Nowicki, J. L., Coley, T. L., Barber, R. T., Lindley, S., Watson, A. J., Van Scoy, K., Law, C. S., Liddicoat, M. I., Ling, R., Stanton, T., Stockel, J., Collins, C., Anderson, A., Bidigare, R., Ondrusek, M., Latasa, J., Millero, F. J., Lee, K., Yao, W., Zhang, J.-Z., Friederich, G., Sakamoto, C., Chavez, F., Buck, K., Kolber, Z., Greene, R., Falkowski, P., Chisholm, S. W., Hoge, F., and Tindale, N. W.: Testing the iron hypothesis in ecosystems of the equatorial Pacific Ocean, Nature, 371, 123–129, https://doi.org/10.1038/371123a0, 1994.

Martin, J. H., Fitzwater, S. E.: Iron deficiency limits phytoplankton growth in the north-east Pacific subarctic, Nature, 331, 341–343, https://doi.org/10.1038/331341a0, 1988.

Maters, E. C., Delmelle, P., Bonneville, S.: Atmospheric processing of volcanic glass: Effects on iron solubility and redox speciation, Environ. Sci. Technol., 50, 5033–5040, https://doi.org/10.1021/acs.est.5b06281, 2016.

Meskhidze, N., Chameides, W. L., Nenes, A.: Dust and pollution: A recipe for enhanced ocean fertilization? J. Geophys. Res., 110, D03301, https://doi.org/10.1029/2004JD005082, 2005.

Miyamoto, C., Sakata, K., Yamakawa, Y., Takahashi, Y.: Determination of calcium and sulfate species in aerosols associated with the conversion of its species through reaction processes in the atmosphere and its influence on cloud condensation nuclei activation, Atmos. Environ., 223, 117193, https://doi.org/10.1016/j.atmosenv.2019.117193, 2020.

Morton, P. L., Landing, W. M., Hsu, S. C., Milne, A., Aguilar-Islas, A. M., Baker, A. R. Methods for the sampling and analysis of marine aerosols: results from the 2008 GEOTRACES aerosol intercalibration experiment.: Limnol. Oceanogr. Methods, 11, 62–78, https://doi.org/10.4319/lom.2013.11.62, 2013.

Muhs, D. R.: The geologic records of dust in the Quaternary, Aeolian Res., 9, 3–48, https://doi.org/10.1016/j.aeolia.2012.08.001, 2013.

Oakes, M., Ingall, E. D., Lai, B., Shafer, M. M., Hays, M. D., Liu, Z. G., Russell, A. G., and Weber, R. J.: Iron solubility related to particle sulfur content in source emission and ambient fine particles, Environ. Sci. Technol., 46, 6637–6644, https://doi.org/10.1021/es300701c, 2012.

Olgun, N., Duggen, S., Croot, P. L., Delmelle, P., Dietze, H., Schacht, U.: Surface ocean iron fertilization: The role of airborne volcanic ash from subduction zone and hot spot volcanoes and related iron fluxes into the Pacific Ocean, Global Biogeochem. Cycles, 36, GB4001, https://doi.org/10.1029/2009GB003761, 2011.

https://doi.org/10.5194/egusphere-2026-1613
Preprint. Discussion started: 8 April 2026

Paris, R., Desboeufs, K. V.: Effect of atmospheric organic complexation on iron-bearing dust solubility, Atmos. Chem. Phys., 13, 4895–4905, https://doi.org/10.5194/acp-13-4895-2013, 2013.

Paris, R., Desboeufs, K. V., Journet, E.: Variability of dust iron solubility in atmospheric waters: Investigation of the role of oxalate organic complexation, Atmos. Environ., 45, 6510−6517, https://doi.org/10.1016/j.atmosenv.2011.08.068, 2011.

Patey, M. D., Achterberg, E. P., Rijkenberg, M. J., Pearce, R.: Aerosol time-series measurements over the tropical Northeast Atlantic Ocean: Dust sources, elemental composition and mineralogy, Mar. Chem., 174, 103–119, https://doi.org/10.1016/j.marchem.2015.06.004, 2015.

Perron, M. M. G., Proemse, B. C., Strzelec, M., Gault-Ringold, M., Boyd, P. W., Rodriguez, E. S., Paull, B., and Bowie, A. R.: Origin, transport and deposition of aerosol iron to Australian coastal waters, Atmos. Environ., 228, 117432, https://doi.org/10.1016/j.atmosenv.2020.117432, 2020a.

Perron, M. M. G., Proemse, B. C., Strzelec, M., Gault-Ringold, M., Bowie, A. R.: Atmospheric inputs of volcanic iron around Heard and McDonald Islands, Southern ocean, Environ. Sci. Atmos., 1, 508, https://doi.org/10.1039/D1EA00054C, 2021.

Perron, M. M. G., Strzelec, M., Gault-Ringold, M., Proemse, B. C., Boyd, P. W., Bowie, A. R.: Assessment of leaching protocols to determine the solubility of trace metals in aerosols, Talanta, 208, 120377, https://doi.org/10.1016/j.talanta.2019.120377, 2020b.

Pye, H. O. T., Nenes, A., Alexander, B., Ault, A. P., Barth, M. C., Clegg, S. L., Collett Jr., J. L., Fahey, K. M., Hennigan, C. J., Herrmann, H., Kanakidou, M., Kelly, J. T., Ku, I.-T., McNeill, V. F., Riemer, N., Schaefer, T., Shi, G., Tilgner, A., Walker, J. T., Wang, T., Weber, R., Xing, J., Zaveri, R. A., and Zuend, A.: The acidity of atmospheric particles and clouds, Atmos. Chem. Phys., 20, 4809–4888, https://doi.org/10.5194/acp-20-4809-2020, 2020.

Rathod, S. D., Hamilton, D. S., Mahowald, N. M., Klimont, Z., Vorbett, J. J., Bond, T. C.: A mineralogy-based anthropogenic combustion-iron emission inventory, J. Geophys. Res. Atmos., 125, e2019JD032114, https://doi.org/10.1029/2019JD032114, 2020.

Rathod, S. D., Hamilton, D. S., Nino, L. L., Kreidenweis, S. M., Bian, Q., Mahowald, N. M., Alastuey, A., Querol, X., Paytan, A., Artaxo, P., Herut, B., Gaston, C., Prospero, J., Chellam, S., Hueglin, C., Varrica, D., Dongarra, G., Cohen, D. D., Smichowski, P., Gomez, D., Lambert, F., Barraza, F., Bergametti, G., Rodríguez, S., Gonzalez-Ramos, Y., Hand, J., Kyllönen, K., Hakola, H., Chuang, P. Y., Hopke, P. K., Harrison, R. M., Martin, R. V., Walsh, B., Weagle, C., Maenhaut, W., Morera-Gómez, Y., Chen, Y. C., Pierce, J. R., and Bond, T. C.: Constraining present-day anthropogenic total iron emission using model and observations, J. Geophys. Res. Atmos., 129, e2023JD040332, https://doi.org/10.1029/2023JD040332, 2024.

Rudnick, R. L., Gao, S. Composition of the continental crust.: Treatise on Geochemistry, 3, 1–64, 2003.

Sakata, K., Kurisu, M., Takeichi, Y., Sakaguchi, A., Tanimoto, H., Tamenori, Y., Matsuki, A., and Takahashi, Y.: Iron (Fe) speciation in size-fractionated aerosol particles in the Pacific Ocean: The role of organic complexation of Fe with humic-like substances in controlling Fe solubility, Atmos. Chem. Phys., 22, 9461–9482, https://doi.org/10.5194/acp-22-9461-2022, 2022.

Sakata, K., Kurisu, M., Tanimoto, H., Sakaguchi, A., Uematsu, M., Miyamoto, C., Takahashi, Y.: Custom-made PTFE filters for ultra-clean size-fractionated aerosol sampling for trace metals, Mar. Chem., 206, 100– 108, https://doi.org/10.1016/j.marchem.2018.09.009, 2018.

Sakata, K., Sakaguchi, A., Yamakawa, Y., Miyamoto, C., Kurisu, M., Takahashi, Y.: Measurement report: Stoichiometry of dissolved iron and aluminum as an indicator of the factors controlling the fractional solubility of aerosol iron – results of the annual observations of size-fractionated aerosol particles in Japan, Atmos. Chem. Phys., 23, 9815–9836, https://doi.org/10.5194/acp-23-9815-2023, 2023.

Sakata, K., Takano, S., Matsuki, A., Takeichi, Y., Tanimoto, H., Sakaguchi, A., Kurisu, M., and Takahashi, Y.: Atmospheric chemistry in East Asia determines the iron solubility of aerosol particles supplied to the North Pacific Ocean, Atmos. Chem. Phys., 25, 11087–11107, https://doi.org/10.5194/acp-25-11087-2025, 2025.

Schroth, A. W., Crusius, J., Sholkovitz, E. R., Bostick, B. C.: Iron solubility driven by speciation in dust sources to the ocean, Nat. Geosci., 2, 337–340, https://doi.org/10.1038/ngeo501, 2009.

https://doi.org/10.5194/egusphere-2026-1613
Preprint. Discussion started: 8 April 2026

Sedwick, P. N., Sholkovitz, E. R., Church, T. M.: Impact of anthropogenic combustion emissions on the fractional solubility of aerosol iron: Evidence from the Sargasso Sea, Geochem. Geophys. Geosyst., 8, Q10Q06, https://doi.org/10.1029/2007GC001586, 2007.

Seo, H., Kim, G.: Anthropogenic iron invasion into the ocean: Results from the East Sea (Japan Sea), Environ. Sci. Technol., 57, 10745–10753, https://doi.org/10.1021/acs.est.3c01084, 2023.

Shah, V., Jacob. D. J., Moch, J. M., Wang, X., Zhai, S.: Global modeling of cloud water acidity precipitation acidity, and acid inputs to ecosystems, Atmos. Chem. Phys., 20, 12223–12245, https://doi.org/10.5194/acp-20-12223-2020, 2020.

Shelley, R. U., Landing, W. M., Ussher, S. J., Planquette, H., Sarthou, G.: Regional trends in the fractional solubility of Fe and other metals from North Atlantic aerosols (GEOTRACES cruises GA01 and GA03) following a two-stage leach, Biogeosci., 15, 2271–2288, https://doi.org/10.5194/bg-15-2271-2018, 2018.

Shi, Z. B., Woodhouse, M. T., Carslaw, K. S., Krom, M. D., Mann, G. W., Baker, A. R., Savov, I., Fones, G. R., Brooks, B., Drake, N., Jickells, T. D., and Benning, L. G.: Minor effect of physical size sorting on iron solubility of transported mineral dust, Atmos. Chem. Phys., 11, 8459–8469, https://doi.org/10.5194/acp-11-8459-2011, 2011a.

Shi, Z., Bonneville, S., Krom, M. D., Carslaw, K. S., Jickells, T. D., Baker, A. R., Benning, L. G.: Iron dissolution kinetics of mineral dust at low pH during simulated atmospheric processing, Atmos. Chem. Phys., 11, 995–1007, https://doi.org/10.5194/acp-11-995-2011, 2011b.

Shi, Z., Krom, M. D., Bonneville, S., Benning, L. G.: Atmospheric processing outside clouds increases soluble iron in mineral dust, Environ. Sci. Technol., 49, 1472–1477, https://doi.org/10.1021/es504623x, 2015.

Sholkovitz, E. R., Sedwick, P. N., Church, T. M., Baker, A. R., Powell, C. F.: Fractional solubility of aerosol iron: Synthesis of a global-scale data set, Geochimica Cosmochimica Acta, 89, 173–189, https://doi.org/10.1016/j.gca.2012.04.022, 2012.

Sholkovitz, E. R., Sedwick, P. N., Church, T. M.: Influence of anthropogenic combustion emissions on the deposition of soluble aerosol iron to the ocean: Empirical estimates for island sites in th4e North Atlantic, Geochimica Cosmochimica Acta, 73, 3981–4003, 2009.

Shupert, L. A., Ebbs, S. D., Lawrence, J., Gibson, D. J., Filip, P.: Dissolution of copper and iron from automotive brake pad wear debris enhances growth and accumulation by the invasive macrophyte Salvinia molesta Mitchell, Chemosphere, 92, 45–51, https://doi.org/10.1016/j.chemosphere.2013.03.002, 2013.

Song, Q., Osada, K.: Seasonal variation of aerosol acidity in Nagoya, Japan and factors affecting it, Atmos. Environ. X, 5, 100062, https://doi.org/10.1016/j.aeaoa.2020.100062, 2020.

Song, Q., Zhang, Z., Yu, H., Ginoux, P., Shen, J.: Global dust optical depth climatology derived from CALIOP and MODIS aerosol retrievals on decadal timescales: regional and interannual variability, Atmos. Chem. Phys., 21, 13369–13395, https://doi.org/10.5194/acp-21-13369-2021, 2021.

Sullivan, R. C., Guazzotti, S. A., Sodeman, D. A., Prather, K. A.: Direct observations of the atmospheric processing of Asian mineral dust, Atmos. Chem. Phys., 7, 1213–1236, https://doi.org/10.5194/acp-7-1213-2007, 2007.

Takahashi, Y., Furukawa, T., Kanai, Y., Uematsu, M., Zheng, G., Marcus, M. A.: Seasonal changes in Fe species and soluble Fe concentration in the atmosphere in the Northwest Pacific region based on the analysis of aerosols collected in Tsukuba, Japan, Atmos. Chem. Phys., 13, 7695–7710, https://doi.org/10.5194/acp-13-7695-2013, 2013.

Takahashi, Y., Higashi, M., Furukawa, T., Mitsunobu, S.: Change of iron species and iron solubility in Asian dust during the long-range transport from western China to Japan, Atmos. Chem. Phys., 11, 11237–11252, https://doi.org/10.5194/acp-11-11237-2011, 2011.

Takahashi, Y., Miyoshi, T., Higashi, M., Kamioka, H., Kanai, Y.: Neutralization of calcite in mineral aerosols by acidic sulfur species collected in China and Japan studied by Ca K-edge X-ray absorption near-edge structure, Environ. Sci. Technol., 43, 6535–6540, https://doi.org/10.1021/es9010256, 2009.

Tao, Y., Murphy, J. G.: The sensitivity of PM2.5 acidity to meteorological parameters and chemical composition changes: 10-year records from six Canadian monitoring sites, Atmos. Chem. Phys., 19, 9309–9320, https://doi.org/10.5194/acp-19-9309-2019, 2019a.

https://doi.org/10.5194/egusphere-2026-1613
Preprint. Discussion started: 8 April 2026

Tao, Y., Murphy, J. G.: The mechanisms responsible for the interactions among oxalate, pH, and Fe dissolution in $PM_{2.5}$, ACS Earth Space Chem., 3, 2259−2265, https://doi.org/10.1021/acsearthspacechem.9b00172, 2019b.

Taylor, S. R. Abundance of chemical elements in the continental crust: a new table.: Geochimica Cosmochimica Acta, 28, 1273–1285, https://doi.org/10.1016/0016-7037(64)90129-2, 1964.

Taylor, S. R., McLennan, S. M.: The geochemical evolution of the continental crust, Rev. Geophys., 33, 241–265, https://doi.org/10.1029/95RG00262, 1995.

Turekian, K. K., Wedepohl, K. H.: Distribution of the elements in some major units of the Earth's crust, Geological Society of American Bulletin, 72, 175–192, https://doi.org/10.1130/0016-7606(1961)72[175:DOTEIS]2.0.CO,2, 1961.

Uematsu, M., Duce, R. A., Prospero, J. M., Chen, L., Merrill, J. T., McDonald, R. L.: Transport of mineral aerosol from Asia over the North Pacific ocean, J. Geophys. Res., 88, 5342–5352, https://doi.org/10.1029/jc088ic09p05343, 1983.

van der Does, M., Brummer, G. J. A., Korte, L. F., Stuut, J. B. W.: Seasonality in Saharan dust across the Atlantic Ocean: From atmospheric transport to seafloor deposition, J. Geophys. Res. Atmos., 126, e2021JD034614, https://doi.org/10.1029/2021JD034614, 2021.

Varela-Lopes, G. E., Molion, L. C. B.: Precipitation patterns in Cape Verde Islands: Santiago Island case study, Atmos. Clim. Sci., 4, 854–865, https://doi.org/10.4236/acs.2014.45075, 2014.

Wedepohl, K. H The composition of the continental crust.: Geochimica Cosmochimica Acta, 59, 1217–1232, https://doi.org/10.1016/0016-7037(95)00038-2, 1995.

Winton, V. H. L., Edwards, R., Bowie, A. R., Keywood, M., Williams, A. G., Chambers, S. D., Selleck, P. W., Desservettaz, M., Mallet, M. D., and Paton-Walsh, C.: Dry season aerosol iron solubility in tropical northern Australia, Atmos. Chem. Phys., 16, 12829–12848, https://doi.org/10.5194/acp-16-12829-2016, 2016.

Wu, H. Y., Hsieh, C. C., Ho, T. Y.: Trace metal dissolution kinetics of East Asian size-fractionated aerosols in seawater: The effect of a model siderophore, Mar. Chem., 254, 104277, https://doi.org/10.1016/j.marchem.2023.104277, 2023.

Yoon, J. E., Son, S., Kim, I. N.: Capture of decline in spring phytoplankton biomass derived from COVID-19 lockdown effect in the Yellow Sea offshore waters, Mar. Pollut. Bull., 174, 113175, https://doi.org/10.1016/j.marpolbul.2021.113175, 2022.

Yu, H., Tan, Q., Chin, M., Remer, L. A., Kahn, R. A., Bian, H., Kim, D., Zhang, Z., Yuan, T., Omar, A. H., Winker, D. M., Levy, R., Kalashnikova, O., Crepeau, L., Capelle, V., and Chedin, A.: Estimates of African dust deposition along the trans-Atlantic transit using the decadelong record of aerosol measurements from CALIOP, MODIS, MISR, and IASI, J. Geophys. Res. Atmos., 124, 7975–7996, https://doi.org/10.1029/2019JD030574, 2019.

Zhang, J., Zhou, X., Wang, Z., Yang, L., Wang, J., Wang, W. Trace elements in $PM_{2.5}$ in Shandong Province: Source identification and health risk assessment.: Sci. Total Environ., 621, 558–577, https://doi.org/10.1016/j.scitotenv.2017.11.292, 2018.

Zheng, G., Su, H., Wang, S., Andreae, M. O., Pöschl, U., Cheng, Y.: Multiphase buffer theory explains contrasts in atmospheric aerosol acidity, Science, 369, 1374–1377, https://doi.org/10.1126/science.aba3719, 2020.

Zhu, Q., Liu, Y., Shao, T., Tang, Y.: Transport of Asian aerosols to the Pacific Ocean, Atmos. Res., 234, 104735, https://doi.org/10.1016/j.atmosres.2019.104735, 2020.

Zhu, Y., Li, W., Wang, Y., Zhang, J., Liu, L., Xu, L., Xu, J., Shi, J., Shao, L., Fu, P., Zhang, D., and Shi, Z.: Sources and processes of iron aerosols in a megacity in Eastern China, Atmos. Chem. Phys., 22, 2191–2202, https://doi.org/10.5194/acp-22-2191-2022, 2022.